

1 Interactions between main-channels and 2 tributary alluvial fans: channel 3 adjustments and sediment-signal 4 propagation

5 Sara Savi¹, Stefanie Tofelde^{1,2}, Andrew D. Wickert³, Aaron Bufe², Taylor F. Schildgen^{1,2}, and
6 Manfred R. Strecker¹

7 ¹Institut für Geowissenschaften, Universität Potsdam, 14476 Potsdam, Germany

8 ²Helmholtz Zentrum Potsdam, GeoForschungsZentrum (GFZ) Potsdam, 14473 Potsdam,
9 Germany

10 ³Department of Earth Sciences and Saint Anthony Falls Laboratory, University of Minnesota,
11 Minneapolis, MN 55455, USA

12 Corresponding Author: Sara Savi (savi@geo.uni-potsdam.de)

13

14 Abstract

15 Climate and tectonics impact water and sediment fluxes to fluvial systems. These boundary
16 conditions set river form and can be recorded by fluvial deposits. Reconstructions of boundary
17 conditions from these deposits, however, is complicated by complex channel-network
18 interactions and associated sediment storage and release through the fluvial system. To address
19 this challenge, we used a physical experiment to study the interplay between a main channel and
20 a tributary under different forcing conditions. In particular, we investigated the impact of a single
21 tributary junction, where sediment supply from the tributary can produce an alluvial fan, on
22 channel geometries and associated sediment-transfer dynamics. We found that the presence of an
23 alluvial fan may either promote or prevent sediment to be moved within the fluvial system,
24 creating different coupling conditions. By analysing different environmental scenarios, our
25 results reveal the contribution of both the main channel and the tributary to fluvial deposits

26 upstream and downstream of the tributary junction. We summarize all findings in a new
27 conceptual framework that illustrates the possible interactions between tributary alluvial fans and
28 a main channel under different environmental conditions. This framework provides a better
29 understanding of the composition and architecture of fluvial sedimentary deposits found at
30 confluence zones, which can facilitate the reconstruction of the climatic or tectonic history of a
31 basin.

32 1. Introduction

33 The geometry of channels and the downstream transport of sediment and water in rivers are
34 determined by climatic and tectonic boundary conditions (Allen, 2008, and references therein).
35 Fluvial deposits and landforms such as conglomeratic fill terraces or alluvial fans may record
36 phases of aggradation and erosion that are linked to changes in sediment or water discharge, and
37 thus provide important archives of past environmental conditions (Armitage et al., 2011;
38 Castelltort and Van Den Driessche, 2003; Densmore et al., 2007; Mather et al., 2017; Rohais et
39 al., 2012; Tofelde et al., 2017). Tributaries are an important component of fluvial networks, but
40 their contribution to the sediment supply of a river channel can vary substantially (Bull, 1964;
41 Hooke, 1967; Lane 1955; Leopold and Maddock, 1953; Mackin, 1948; Miller, 1958). Their
42 impact on the receiving river (referred to as *main channel* hereafter) may not be captured by
43 numerical models of alluvial channels, as most models either parameterize the impacts of
44 tributaries into simple relationships between drainage-basin area and river discharge (Whipple
45 and Tucker, 2002; Wickert and Schildgen, 2019), or treat the main channel as a single channel
46 with no lateral input (e.g., Simpson and Castelltort, 2012). Extensive studies on river confluences
47 (e.g., Rice et al., 2008 and references therein) mainly focus on (1) hydraulic parameters of the
48 water flow dynamics at the junction (Best 1986, 1988), which are relevant for management of
49 infrastructure (e.g., bridges), and (2) morphological changes of the main channel bed, which are
50 relevant for sedimentological studies and riverine habitats (Benda et al., 2004a; Best 1986; Best
51 and Rhoads, 2008). Geomorphological changes (i.e., channel slope, width, or grain-size
52 distribution) have been studied in steady-state conditions only (Ferguson et al., 2006; Ferguson
53 and Hoey, 2008), and with no focus on fluvial deposits related to the interactions between

54 tributaries and the main channel. In source-to-sink studies an understanding of these processes,
55 however, is relevant for the reconstruction of the climatic or tectonic history of a certain basin.

56 By modulating the sediment supplied to the main channel, tributaries may influence the
57 distribution of sediment within the fluvial system, the duration of sediment transport from source
58 areas to depositional basins (Simpson and Castelltort, 2012), and the origin and amount of
59 sediment stored within fluvial deposits and at confluence zones. Additionally, complex
60 feedbacks between tributaries and main channels (e.g., Schumm, 1973; Schumm and Parker,
61 1973) may enhance or reduce the effects of external forcing on the fluvial system, thus
62 complicating attempts to reconstruct past environmental changes from these sedimentary
63 deposits.

64 The dynamics of alluvial fans can introduce an additional level of complication to the
65 relationship between tributaries and main channels. Fans retain sediment from the tributary and
66 influence the response of the connected fluvial system to environmental perturbations (Ferguson
67 and Hoey, 2008; Mather et al., 2017). Despite the widespread use of alluvial fans to decipher
68 past environmental conditions (Bull, 1964; Colombo et al., 2000; D'Arcy et al., 2017; Densmore
69 et al., 2007; Gao et al., 2018; Harvey, 1996; Savi et al., 2014; Schildgen et al., 2016), we lack a
70 clear understanding of the interactions between alluvial fans and main channels under the
71 influence of different environmental forcing mechanisms. This knowledge gap limits our
72 understanding of (1) how channels respond to changes in water and sediment supply at
73 confluence zones, and (2) how sediment moves within fluvial systems (Mather et al., 2017;
74 Simpson and Castelltort, 2012), with potential consequences for sediment-transport dynamics as
75 well as for the composition and architecture of fluvial sedimentary deposits.

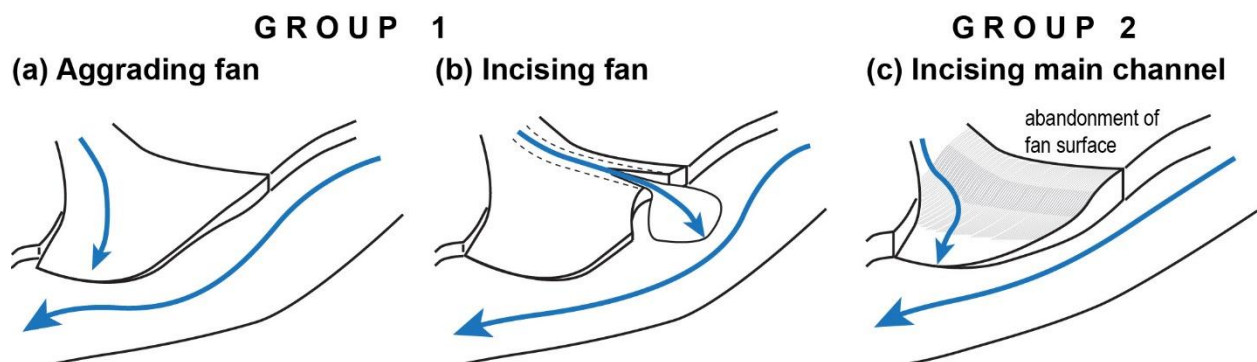
76 In this study, we analyze the interplay between a main channel and a tributary under different
77 environmental forcing conditions in an experimental setting, with particular attention to
78 tributaries that generate an alluvial fan. Physical experiments have the advantage of providing a
79 simplified setting with controlled boundary conditions that may include water and sediment
80 discharge, and uplift rate or base-level changes. These models may thus capture many
81 components of complex natural behaviors (Hooke, 1967; Paola et al., 2009; Schumm and Parker,
82 1973), and they provide an opportunity to analyze processes at higher spatial and temporal

83 resolution than is generally possible in nature (e.g., De Haas et al., 2016; Parker, 2010; Reitz et
84 al., 2010) and to directly observe connections between external perturbations (e.g., tectonic or
85 climatic variations) and surface processes impacting landscapes.

86 We present results from two groups of experiments in which we separately imposed a
87 perturbation either in the tributary only (Group 1, Fig. 1a, b) or solely in the main channel
88 (Group 2, Fig. 1c). Group 1 can be further subdivided into cases in which the tributary has: (a) an
89 aggrading alluvial fan (Fig. 1a) or (b) an incising alluvial fan (Fig. 1b). In this context, we
90 distinguish between two modes of fan construction: *fan aggradation*, i.e., deposition of material
91 on the fan surface, which leads to an increase in the fan surface elevation, and *fan progradation*,
92 i.e., deposition that occurs at the downstream margin of the fan, which leads to fan lengthening.
93 Progradation may occur during both aggradation and incision phases (Fig. 1). Group 2, in
94 contrast, represents the case of a sudden increase in water discharge in the main channel (Fig.
95 1c), as for example related to an increase in glacial melt.

96 By analyzing how a tributary may affect the main channel under these different forcing
97 conditions, we aim to build a conceptual framework that lends insight into the interplay between
98 alluvial fans and main channels. Toward this goal, we provide a schematic representation of how
99 the downstream delivery of sediment changes under different environmental conditions. Through
100 this representation, we hope to contribute to a better understanding and interpretation of fluvial
101 morphologies and sedimentary records, which may hold important information about regional
102 climatic and tectonic history (Allen, 2008; Armitage et al., 2011; Castelltort and Van Den
103 Driessche, 2003; Densmore et al., 2007; Mather et al., 2017; Rohais et al., 2012).

104



105

106 Figure 1. Schematic representation of the three scenarios analyzed in this study.

107

108 2. Background

109 2.1. Geometry and sediment transfer dynamics in a single-channel system

110 An alluvial river is considered to be in steady state when its water discharge provides
111 sufficient power, or sediment-transport capacity, to transport the sediment load supplied from the
112 upstream contributing area at a given channel slope (Bull, 1979; Gilbert, 1877; Lane, 1955;
113 Mackin, 1948). When a perturbation occurs in the system, the river must transiently adjust one or
114 more of its geometric features (e.g., slope, width, depth, or grain-size distribution) to re-establish
115 equilibrium (Mackin 1948; Meyer-Peter and Müller, 1948). Slope adjustments are not uniform
116 along the channel. If the perturbation occurs in the basin's headwater (e.g., a change in water or
117 sediment supply), slope adjustments propagate downstream from the channel head (Simpson and
118 Castellort 2012; Tofelde et al., 2019; Van den Berg Van Saparoea and Potsma, 2008; Wickert
119 and Schildgen, 2019). In contrast, slope adjustments propagate upstream if a perturbation occurs
120 toward the downstream end of the channel (e.g., a change in base level) (Parker et al., 1998;
121 Tofelde et al., 2019; Van den Berg Van Saparoea and Potsma, 2008; Whipple et al., 1998). The
122 sediment transport rate of the river also depends on the direction of the change, as an increase or
123 a decrease in precipitation or uplift rates trigger opposite responses (i.e., increase or decrease in
124 sediment transport rate; Bonnet and Crave, 2003).

125 2.2. Geometry and sediment-transfer dynamics in a multi-channel system

126 2.2.1. *Tributary influence on main channel*

127 At confluence zones, the main channel is expected to adapt its width, slope, sediment
128 transport rate, and sediment-size distribution according to the combined water and sediment
129 supply from the main channel and the tributary (Benda et al., 2004b; Best, 1986; Ferguson et al.,
130 2006; Lane 1955; Miller, 1958; Rice et al., 2008). Consequently, a perturbation occurring in the
131 tributary will also affect the main channel. In their numerical model, Ferguson et al. (2006)
132 explored the effects that changes in sediment supplied from a tributary have on the main

133 channel's slope. They found that when tributaries cause aggradation at the junction with the main
134 channel, the main channel slope adjustments extend approximately twice as far upstream as they
135 do downstream. They additionally found that variations in grain size of the tributary influence
136 the grain-size distribution in the main channel, both upstream and downstream of the tributary
137 junction. Because we used a homogeneous grain size in our experiments, the work of Ferguson
138 et al. (2006) complements our analyses.

139 Whether the tributary is aggrading, incising, or in equilibrium may also have important
140 consequences for *how* and *where* local fluvial deposits (i.e., alluvial-fan deposits or fluvial
141 terraces) reflect environmental signals. For example, when sediment is trapped within a
142 tributary's alluvial fan, the fan acts as a *buffer* for the main channel, and environmental signals
143 do not propagate from the tributary into the fluvial deposits of the main channel (Ferguson and
144 Hoey, 2008; Mather et al., 2017). In contrast, where the tributary and main channel are fully
145 *coupled* (i.e. all sediment mobilized in the tributary reaches the main channel), the signal
146 transmitted from the tributary can be recorded in the stratigraphy of the main river (Mather et al.,
147 2017). The presence of an alluvial fan may additionally cause a change in the main river
148 location, pushing it against the opposite side of the valley. This allows the fan to grow more in
149 the downstream direction of the main flow, contributing to a strong asymmetry in its morphology
150 that may be preserved in the stratigraphic record of the flood plain (Giles et al., 2016).

151 2.2.2. *Main channel influence on tributary*

152 The main channel influences a tributary primarily by setting its local base level. Therefore, a
153 change in the main-channel bed elevation through aggradation or incision represents a
154 downstream perturbation for the tributary, and tributary-channel adjustments will follow a
155 *bottom-up* propagation direction (Mather et al., 2017; Schumm and Parker, 1973). Typically, a
156 lowering of the main channel produces an initial phase of tributary-channel incision (Cohen and
157 Brierly, 2000; Fulkner et al., 2016; Germanoski and Ritter, 1988; Heine and Lant, 2009; Ritter et
158 al., 1995; Simon and Rinaldi, 2000), followed by channel widening (Cohen and Brierly, 2000;
159 Germanoski and Ritter, 1988), which occurs through bank erosion and mass-wasting processes
160 (Simon and Rinaldi, 2000). As base-level lowering continues, the fan may become entrenched,
161 with the consequent abandonment of the fan surface and renewed deposition at a lower elevation

162 (Clark et al., 2010; Mather et al., 2017; Mouchené et al., 2017; Nicholas et al., 2009) (Fig. 1c). In
163 contrast, aggradation of the main channel may lead to tributary-channel backfilling and avulsion
164 (Bryant et al., 1995; De Haas et al., 2016; Hamilton et al. 2013; Kim and Jerolmack, 2008; Van
165 Dijk et al., 2009, 2012).

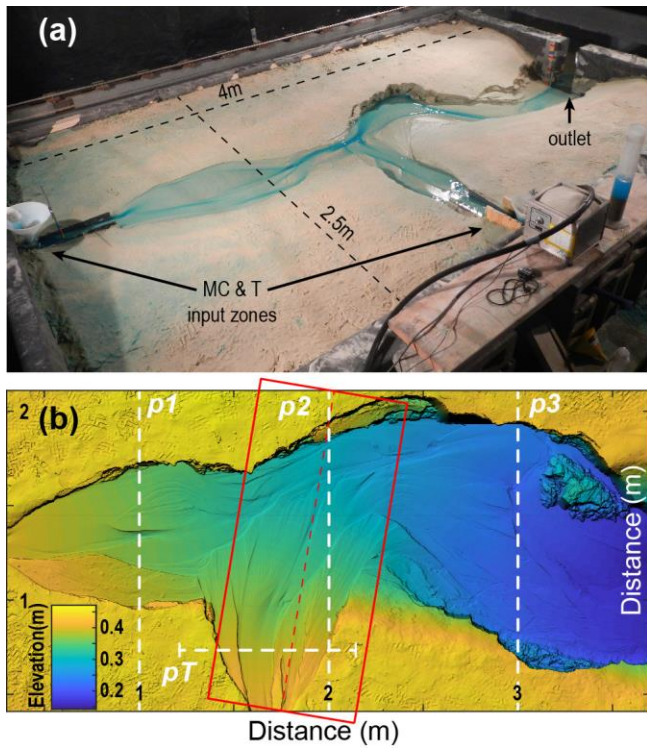
166 When a non-incising main channel (*non-incising main axial river* of Leeder and Mack, 2001)
167 is characterized by efficient lateral erosion, it can efficiently erode the fan downstream margin,
168 thereby “cutting” its toe (Larson et al., 2015) (*fan-toe cutting* hereafter) (Fig. 1b). This toe-
169 cutting generally occurs in the up-valley side of the fan and thus shortens it (Giles et al., 2016.)
170 As a consequence, the tributary channel-slope increases and so does its transport capacity, which
171 triggers an upstream-migrating wave of incision. Fan-toe cutting may thus cause fan incision and
172 a consequent increase in sediment supply from the tributary to the main channel (*healing wedge*
173 hereafter; Leeder and Mack, 2001), in a process similar to that caused by an incising main
174 channel (*incising main axial river of* Leeder and Mack, 2001).

175 3. Methods

176 3.1. Experimental setup

177 We conducted physical experiments at the Saint Anthony Falls Laboratory (Minneapolis,
178 USA). The experimental setup consisted of a wooden box with dimensions of 4 m x 2.5 m x 0.4
179 m, which was filled with quartz sand with a mean grain size of 144 μm (standard deviation of 40
180 μm). Two separate water and sediment input zones were used to form a main channel (MC) and
181 a tributary channel (T) (Fig. 2a). The main channel’s input zone was located along the short side
182 of the box, whereas the tributary’s input zone was located along the long side at a distance of 1.7
183 m downstream of the main-channel inlet (Fig. 2a). This setting represents a landscape with two
184 transport-limited streams that join in a broad alluvial valley of unlithified/uncemented sediments;
185 common for many arid regions with large flood plains. A simplification in our experiments is
186 that the grain sizes from both the main stem and the tributary are equal. This will be further
187 discussed in section 5.4. For each of the two input zones, the water supply (Q_w) and sediment
188 supply (Q_{s_in}) could be regulated separately, and sand and water were mixed before entering the
189 box by feeding them through cylindrical wire-mesh diffusers filled with gravel. Before entering

190 the mesh, water was dyed blue to be visible on photos. At the downstream end, sand (Q_{s_out}) and
 191 water exited the basin through a fix 20 cm-wide gap that opened onto the floor below. This
 192 downstream sink was required to avoid deltaic sediment deposition that would, if allowed to
 193 grow, eventually raise the base level of the fluvial system. At the beginning of each experiment,
 194 an initial channel was shaped by hand to allow the water to flow towards the outlet of the box.



195
 196 Figure 2. Experimental set-up. (a) Wooden box for the experiments showing the two zones of
 197 sediment and water input, and the outlet of the basin. (b) Digital elevation model constructed
 198 from laser scans (1 mm horizontal resolution). Red box shows the area of the swath grid used for
 199 the calculation of the tributary long profile (Fig. 4) and slope values. Dashed white lines
 200 represent the location of the cross sections shown in Figs. 5 and S1 of the Supplementary
 201 Material.

202

203 3.2. Boundary conditions

204 We performed six experiments with different settings and boundary conditions to simulate
 205 different tributary–main-channel interactions (Table 1). As a reference, we included one
 206 experiment without a tributary and with a constant Q_{s_in} and Q_w (MC_NC, where MC stands for

207 *Main Channel only* and the suffix NC stands for *No Change* in boundary conditions; reported in
 208 Tofelde et al., 2019 as the Ctrl_2 experiment). The other five experiments all have a tributary
 209 and are divided into two groups: In Group 1, Q_w and Q_{s_in} on the main channel were held
 210 constant, whereas we varied these inputs to the tributary. In Group 2, Q_w and Q_{s_in} on the
 211 tributary were held constant, whereas we increased Q_w in the main channel. In natural systems,
 212 changes in water and sediment supply may affect the main channel and tributary simultaneously,
 213 but to isolate the effects of the main channel and the tributary on each other, we studied
 214 perturbations that only affect one of them at a time. Our results can be combined to predict the
 215 response to a system-wide change in boundary conditions.

216 Each group includes one experiment with no change (NC) in Q_{s_in} and Q_w (T_NC1 and
 217 T_NC2, where T stands for *run with Tributary* and the numbers at the end correspond to the
 218 group number). Group 1 includes one experiment with an increase followed by a decrease in
 219 Q_{s_in} in the tributary (T_ISDS, where ISDS stands for *Increasing Sediment Decreasing Sediment*)
 220 and one experiment with a decrease followed by an increase in Q_w in the tributary (T_DWIW,
 221 where DWIW stands for *Decreasing Water Increasing Water*). Changes were first made in the
 222 direction that favored sediment deposition and the construction of an alluvial fan. Group 2
 223 includes one experiment with no change (T_NC2) and one with an increase in Q_w in the main
 224 channel (T_IWMC, where IWMC stands for *Increasing Water in Main Channel*). Importantly,
 225 the initial settings of the two groups of experiments are different (Table 1). The Q_{s_in} and Q_w
 226 values were defined based on a set of preliminary test-runs and chosen to balance sediment
 227 transport and sediment deposition. In particular, initial Q_w and Q_{s_in} of Group 2 guarantee a
 228 higher Q_s/Q_w ratio compared to Group 1, so that we could evaluate the effects of a change in the
 229 main-channel regime (from a *non-incising main river* to an *incising main river*) on the tributary
 230 and on sediment-signal propagation. In the context of this coupled tributary–main-channel
 231 system, we explore: 1) the geometric variations that occur in the main channel and in the
 232 tributary (e.g., channel slope and valley geometry); and 2) the downstream delivery of sediment
 233 and sedimentary signals.

234 **Table 1.** Overview of input parameters.

	Initial conditions	1 st change	2 nd change	Run time (spin-up)
--	--------------------	------------------------	------------------------	--------------------

EXP NAME	MC		T		MC	T		T		min
	Qw	Qs_in	Qw	Qs_in	Qw	Qw	Qs_in	Qw	Qs_in	
	mL/s	mL/s	mL/s	mL/s	mL/s	mL/s	mL/s	mL/s	mL/s	
MC_NC**	95	1.3								690 (100)
<i>Non-incising mean axial rivers – Group1</i>					<i>(at 300 min)</i>		<i>(at 375* or 480 min)</i>			
T_NC1	95	1.3	63	2.2						600 (150)
T_ISDS	95	1.3	63	2.2			4.5		2.2	720 (150)
T_DWIW*	95	1.3	63	2.2		31.5		63		690 (150)
<i>Incising mean axial rivers - Group2</i>					<i>(at 180 min)</i>					
T_NC2	63	1.3	41.5	2.2						480 (100)
T_IWMC	63	1.3	41.5	2.2	126					480 (100)

235 * In the T_DWIW run the boundary condition change occurred at 375 min rather than 480 min
236 as in the T_ISDS experiment because fast aggradation that occurred at the tributary input zone
237 risked to overtop the wooden box margins.

238 **, Experiment published by Tofelde et al. (2019).

239

240 3.3. Measured and calculated parameters

241 3.2.1. Long profiles, valley cross-sections, and slope values

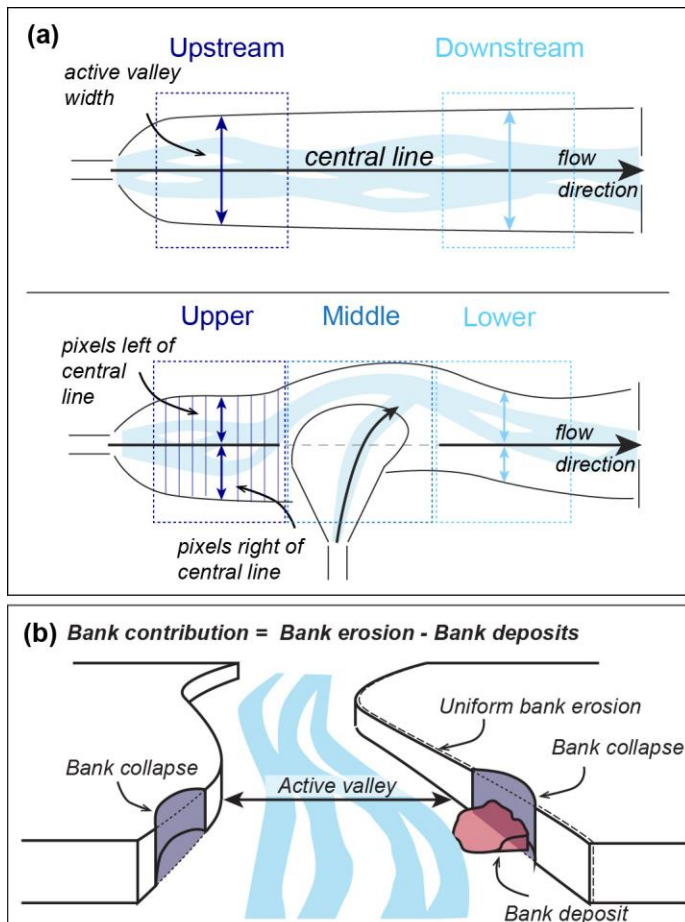
242 Every 30 min we stopped the experiments to perform a scan with a laser scanner mounted
243 on the railing of the basin that surrounded the wooden box. Digital elevation models (DEMs)
244 created from the scans have a resolution of 1 mm (Fig. 2b). We extracted long profiles and valley
245 cross sections from these DEMs (i.e., elevation profiles perpendicular to the main flow direction)
246 for the main channel and the tributary. Long profiles for the main channel were calculated by
247 extracting the lowest elevation point along each cross section in the flow direction. Long profiles
248 for the tributary were calculated with a similar procedure using outputs from Topotoolbox's
249 SWATH profile algorithm (Schwanghart and Scherler, 2014) at 1 mm spatial resolution along
250 the line of the average flow direction (Fig. 2b). By plotting elevation against down-valley or
251 down-fan distance, rather than along the evolving path of the channels, the resulting slopes are
252 slightly overestimated due to the low sinuosity of the channels. Cross sections were extracted at
253 fixed positions, perpendicular to the main flow direction, for both the main channel and the
254 tributary (Fig. 2b).

255 For the main channel, spatially-averaged slopes were additionally calculated by manually
256 measuring the bed elevation at the inlet and at the outlet of the wooden box at 10-minute
257 intervals during the experiments. This procedure yielded real-time estimates of channel slope.
258 For comparison, spatially-averaged slopes were subsequently calculated also for the tributary
259 channel using the maximum and minimum elevation of the tributary long profile calculated
260 within the SWATH grid. Slope data are reported in the supplementary material.

261 3.2.2. *Active valley-floor width and symmetry*

262 We defined the width of the active valley floor as the area along the main channel that was
263 occupied at least once by flowing water. It was measured along the main channel both upstream
264 and downstream of the tributary junction (Fig. 3a, upper panel). The active valley floor was
265 isolated by extracting all DEM values with an elevation of <0.42 m (where 0.42 m is the
266 elevation of the sand surface outside the manually-shaped channel) and with a slope of <15
267 degrees (a value visually selected from the DEMs as the best cut-off value for distinguishing the
268 valley floor from the banks). The average valley-floor width was then calculated as the average
269 sum of pixels in each of the 700 cross sections within the selected zones (i.e., upstream or
270 downstream of the tributary junction; Fig. 3a, upper panel). The same method was used to
271 monitor valley axial symmetry. In this case, the averaged width was limited to the sum of pixels
272 to the left and to the right of an imaginary central line crossing the basin from the inlet to the
273 outlet (Fig. 3a). Small differences between left and right sums indicate high symmetry.

274



275

276 Figure 3. (a) Schematic representation of the method used to calculate the active valley width
 277 and axial symmetry. Symmetry and averaged width values are calculated for 700 cross sections
 278 located within the boxes marked in the upper panel. The averaged position of the valley margins
 279 with respect to an imaginary central line, which connects the source zone to the outlet of the
 280 wooden box, is shown in Figure 6. This representation highlights the symmetry of the valley and
 281 indirectly provides the valley width (i.e., sum of the right and left-margin positions). Boxes
 282 marked in the lower panel show the division into Upper, Middle, and Lower sections used for the
 283 calculation of the mobilized volumes (Fig. 8). (b) Schematic representation of the method used to
 284 calculate bank contribution: Elevation difference > -2.5 cm represents bank erosion and bank
 285 collapses, whereas differences > 2.5 cm represent large bank deposits. The contribution of the
 286 banks is calculated by subtracting these two values.

287

288 3.2.3. Sediment discharge at the outlet (Q_{s_out}), mobilized volumes, and bank
289 contribution

290 The sediment discharge at the outlet of the basin (Q_{s_out}) was manually recorded at 10-minute
291 intervals by measuring the volume of sediment that was collected in a container over a 10-second
292 period. Q_{s_out} was also calculated by differencing subsequent DEMs (generating a “DEM of
293 Difference”, or DoD) and calculating the net change in sediment volume within the DEM.
294 Although having a lower temporal resolution than the manual measurements (i.e., DoDs are
295 averaged over 30 minutes), this DEM-based calculation allowed us to identify zones of
296 aggradation and incision within the system and to calculate their volumes. For each DoD, we
297 distinguished between changes along the active valley floor due to channel dynamics (elevation
298 difference < 2.5 cm, value chosen as best cut-off value) and changes that occur along the channel
299 and valley walls, for example due to bank collapses (elevation difference > 2.5 cm). Changes
300 within the active valley floor were further divided into areas of net *aggradation* ($\Delta V_{vf} > 0$) and
301 net *erosion* ($\Delta V_{vf} < 0$). Changes in bank elevation were divided into net *bank deposition* ($\Delta V_b >$
302 0) and net *bank collapses* or *erosion* ($\Delta V_b < 0$). These were used to calculate the bank
303 contribution (V_b) to the total volume (V) of mobilized sediment (Fig. 3b). We separated the
304 upper, middle, and lower sections of the experimental river valley by dividing the DEMs into
305 three different zones (Fig. 3a, lower panel). For each section, we calculated the net change in
306 sediment volumes between two time steps within the active valley floor (V_{vf}), along the banks
307 (V_b), and the sum of the two contributions ($V = V_{vf} + V_b$).

308 The volumes are normalized to the Q_{s_in} measured over 30 minutes (to match the 30-minute
309 period of a DoD). Negative V values indicate net incision, whereas positive values indicate net
310 aggradation. V values close to zero may indicate that there was no change, or that the net incision
311 \cong net aggradation. As such, it is important to look at the variations through time rather than at
312 single values.

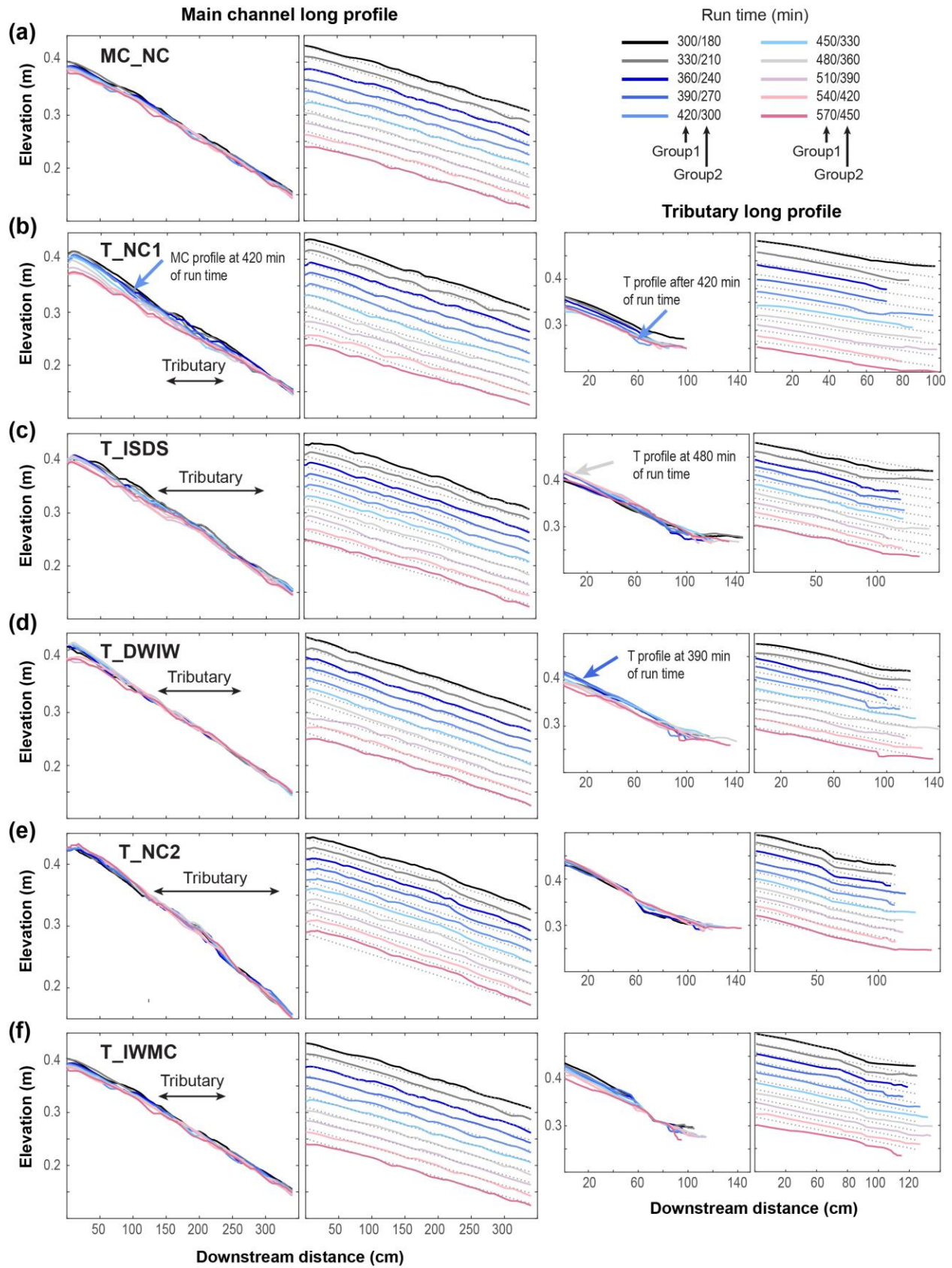
313 4. Results

314 All experiments included an initial adjustment phase characterized by high Q_{s_out} and a
315 short and rapid increase in the main-channel slope through preferential channel incision at the
316 downstream end of the main channel. This phase represents the adjustment from the manually
317 constructed valley shape to the shape that is equilibrated to the imposed boundary conditions. At
318 the start of the adjustment phase, the channel rapidly incised toward the outlet, which was much
319 lower than the height of the manually constructed valley bottom. Meanwhile, the channel
320 deposited material at the channel head, adjusting to the Q_{s_in} and Q_w values. Analogous to a base-
321 level fall observed in nature, these changes caused an increase in main-channel slope near the
322 outlet and the upstream migration of a diffuse knick-zone that lowered the elevation of the main
323 channel. After this initial adjustment, which marks the end of the spin-up phase, the main
324 controlling factors for the shape of the channel were the Q_{s_in} and Q_w values only.

325 4.1. Geometric adjustments

326 Following the spin-up phase, channel-slope adjustments in our experiments matched the
327 theoretical models described above (Section 2.1). The main-channel slope decreased in all
328 experiments through incision at the upstream end, except for T_NC2 and the initial phase of
329 T_IWMC, in which the boundary conditions favored aggradation (Fig. 4, Table 1). The slope of
330 the tributary increased during periods of fan aggradation (e.g., IS phase of the T_ISDS run, and
331 DW phase of the T_DWIW run) and decreased during periods of fan incision (DS phase of the
332 T_ISDS run, and IW phase of the T_DWIW run) (Fig. 4). Slope adjustments did not occur
333 uniformly, but followed a top-down or bottom-up direction depending on the origin of the
334 perturbation (e.g., changes in headwater conditions or base-level fall at the tributary outlet).

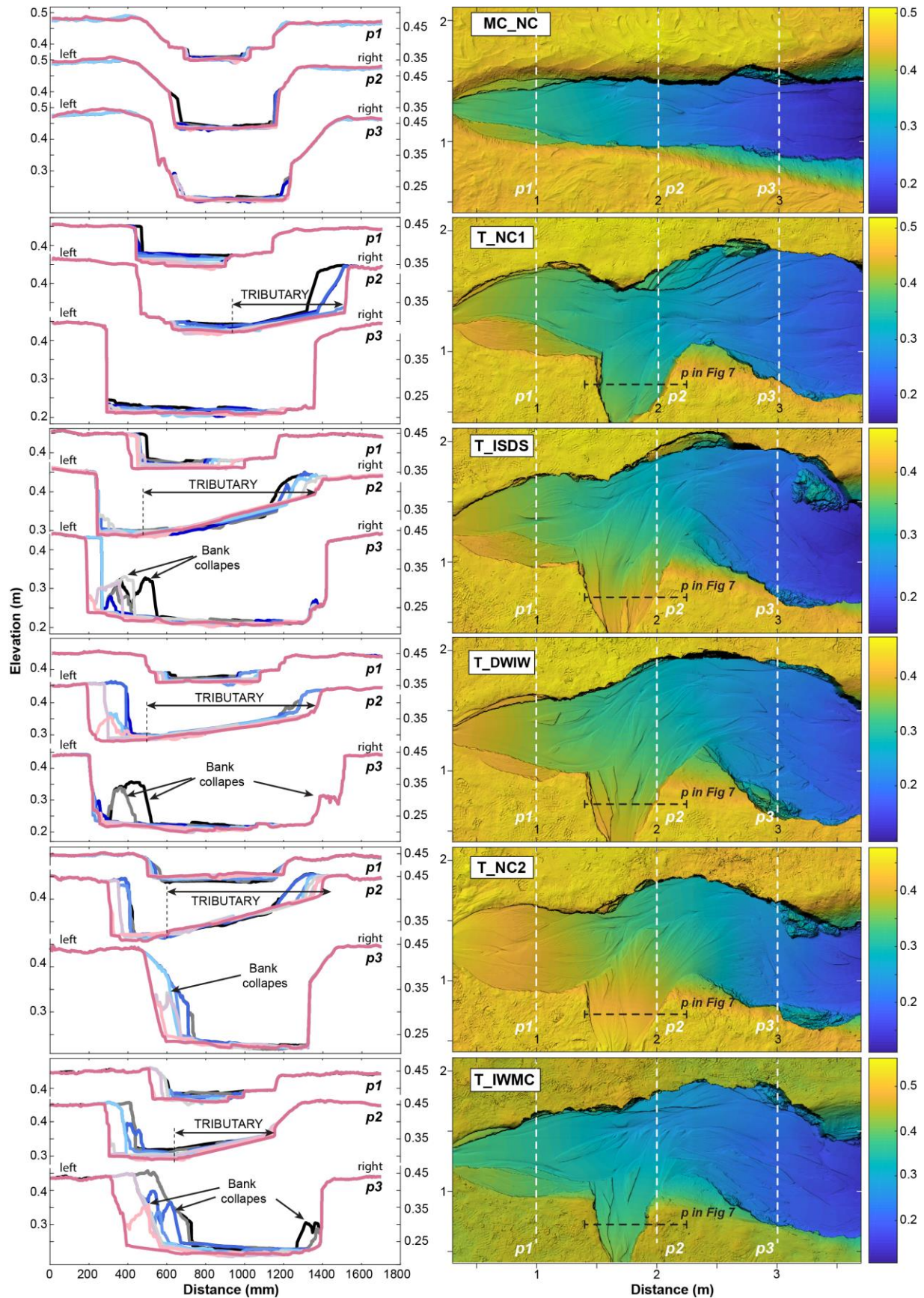
335



337 Figure 4. Long profiles of the main channel (left panels) and of the tributary channel (right
338 panels) for all runs. Profiles represent the experiments between 300 and 570 minutes for the
339 MC_Ctrl2, T_NC1, T_ISDS, and T_DWIW runs (legend values to the left of the slashes), and
340 between 180 and 450 minutes for the T_NC2, and T_IWMC runs (legend values to the right of
341 the slashes). For both the main and the tributary channel, left panels show the topographic
342 evolution of the channels with time, whereas right panels show a single profile (i.e., at a specific
343 time) compared to the average slope of the first plotted profile. Along the main channel profiles,
344 horizontal arrows indicate the position and extent of the tributary channel/alluvial fan, whereas
345 colored arrows indicate the position of the channels in particular run times discussed in the text.
346

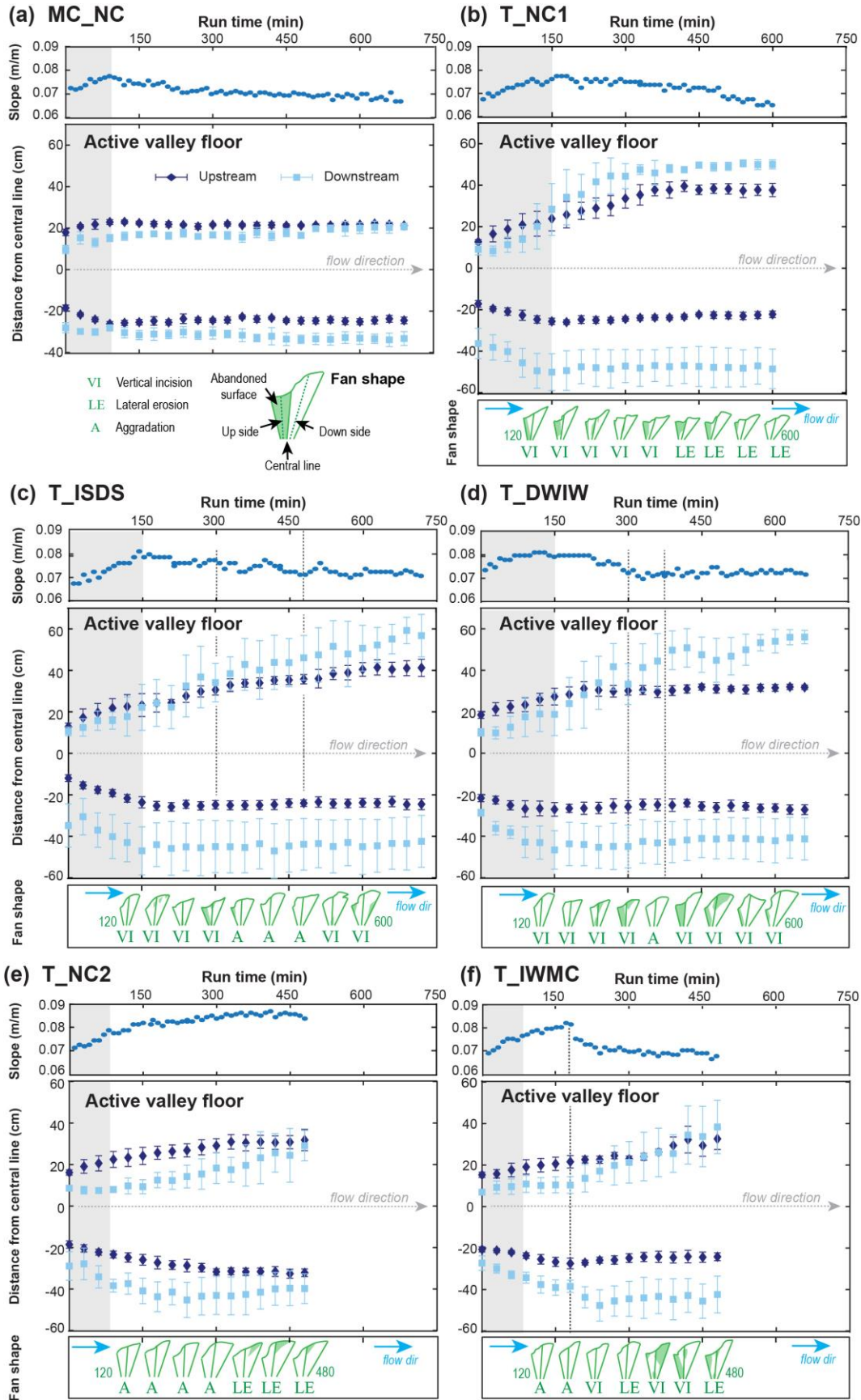
347 Valley width in both the main channel (Fig. 5) and the tributary (Fig. S1 of the
348 Supplementary Material) increased during the experiments through bank erosion and bank
349 collapses, until reaching relatively steady values (Fig. 6). The experiments with the tributary
350 (Fig. 6b – f) developed a much wider main-channel valley, especially downstream of the
351 tributary, due to higher total Q_w compared to the main channel only experiments. In these
352 experiments, valleys were also strongly asymmetrical, with more erosion affecting the valley
353 side opposite the tributary (Figs. 5 and 6).

354



356 Figure 5. Left panels: Cross sections obtained from the DEMs at three different locations along
357 the main channel (p1, p2, and p3 respectively). The color code represents successive DEMs as
358 illustrated in Fig. 4 (i.e., same colors for the same run times). All cross sections are drawn from
359 left to right looking in the downstream direction. Right panels: DEM maps expressed in meters;
360 color code represents the elevation with respect to the channel floor (also in meters).

361



363 Figure 6. Variations in the geometry of the active valley floor for all experiments. For each
364 experiment the upper panel shows the measured slope (measured every 10 minutes during each
365 experimental run). The middle panel shows the calculated average position of the right and left
366 valley margins with respect to the central line, respectively for the main channel upstream and
367 downstream of the tributary junction (as indicated in Fig. 3a). Gray areas represent the spin-up
368 phase of each experiment (based on the break-in-slope registered through the manual slope
369 measurements; (a–f) upper panels). Vertical dotted lines in the T_ISDS, T_DWIW, and
370 T_IWMC runs represent the *time of change* in boundary conditions. Values are reported with
371 their relative 1σ value. For all experiments with a tributary, the shape of the fan and the dominant
372 sedimentary regime acting in the tributary at that specific time (i.e., vertical incision (VI), lateral
373 erosion (LE), or aggradation (A)) are shown in the lower panel. In all experiments, fan-toe
374 cutting (Leeder and Mack, 2001; Larson et al., 2015) mainly occurred at the upstream margin of
375 the fan and contributed to the strong asymmetry of the fan morphology (Table S9 of Supp.
376 Material), similar to what has been observed in nature (Giles et al., 2016).

377

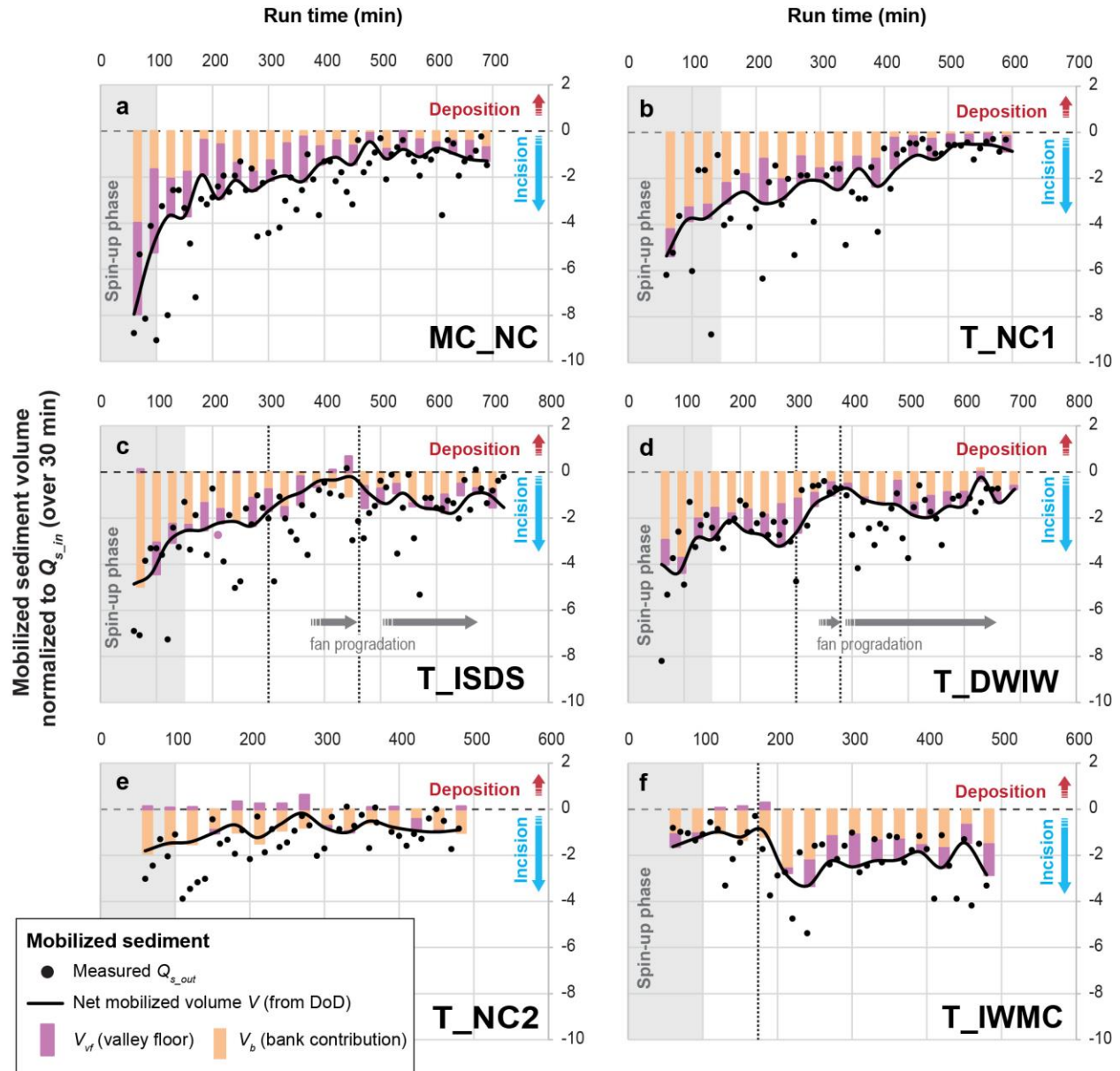
378 4.2. Q_{s_out} and bank contribution

379 Our experiments offered an opportunity to evaluate the impacts of sediment supply from the
380 tributary to the main channel through space and time. In general, sediment moved in pulses, and
381 areas of deposition and incision commonly coexisted (Fig. 7a).

382 Q_{s_out} varied greatly, but generally decreased through time (the only exception is the
383 T_IWMC run, where Q_{s_out} remained high) (Fig. 7, black circles). Values for the mobilized
384 sediment, V , calculated from the DoDs (averaged over 30 minutes) show similar trends, but with
385 a lower variability that reflects the long-term average Q_{s_out} (Fig. 7, black lines). An appreciable
386 reduction of Q_{s_out} occurred when the system was approaching equilibrium (e.g., end of Fig. 7a,
387 b) and during times of fan aggradation in the tributary (i.e., IS and DW phases of Fig. 7c, d, and
388 e). Net mobilized sediment volumes (V) increased again during phases of fan incision (i.e., DS
389 and IW phases of Fig. 7c and d) and main-channel incision (e.g., IW phase in Fig. 7f). These
390 increases were due to the combined effect of a general increase in sediment mobility within the
391 active valley floor (V_{vf}) and lateral erosion of the banks (V_b) (Fig. 7, violet and orange bars
392 respectively, and Fig. S8 of the Supp. Material). The DoD analysis also indicates that in all
393 experiments, with the only exception of the MC run and of the phases approaching steady-state,
394 bank contribution was higher or of the same order of magnitude of the volume mobilized in the
395 valley floor (Fig. 7, orange and violet bars). This observation suggests that bank erosion
396 represented a major contribution to Q_{s_out} (Tables S3 to S8 of Supp. Material) and is particularly

397 true for the T_NC2 run, where aggradation was favored, in which Q_{s_out} is dominated by the
 398 contribution of the banks (Fig. 7e, and Fig. S9 of the Supp. Material).

399



400

401 Figure 7. Volumes of sediment mobilized within the system. Black line: Net mobilized volume
 402 of sediment measured using the DoD. For comparison, black dots represent the Q_{s_out} values
 403 measured every 10 minutes (part of the difference between measured and calculated Q_{s_out} values
 404 may be due to the contribution of the most downstream area of the wooden box, which was
 405 shielded in the DEM reconstruction). Horizontal arrows indicate the timespan of fan
 406 progradation either during fan aggradation or fan incision. Vertical pointed lines represent the
 407 *time of change* in boundary conditions; horizontal dashed line separates aggradation and erosion.

408

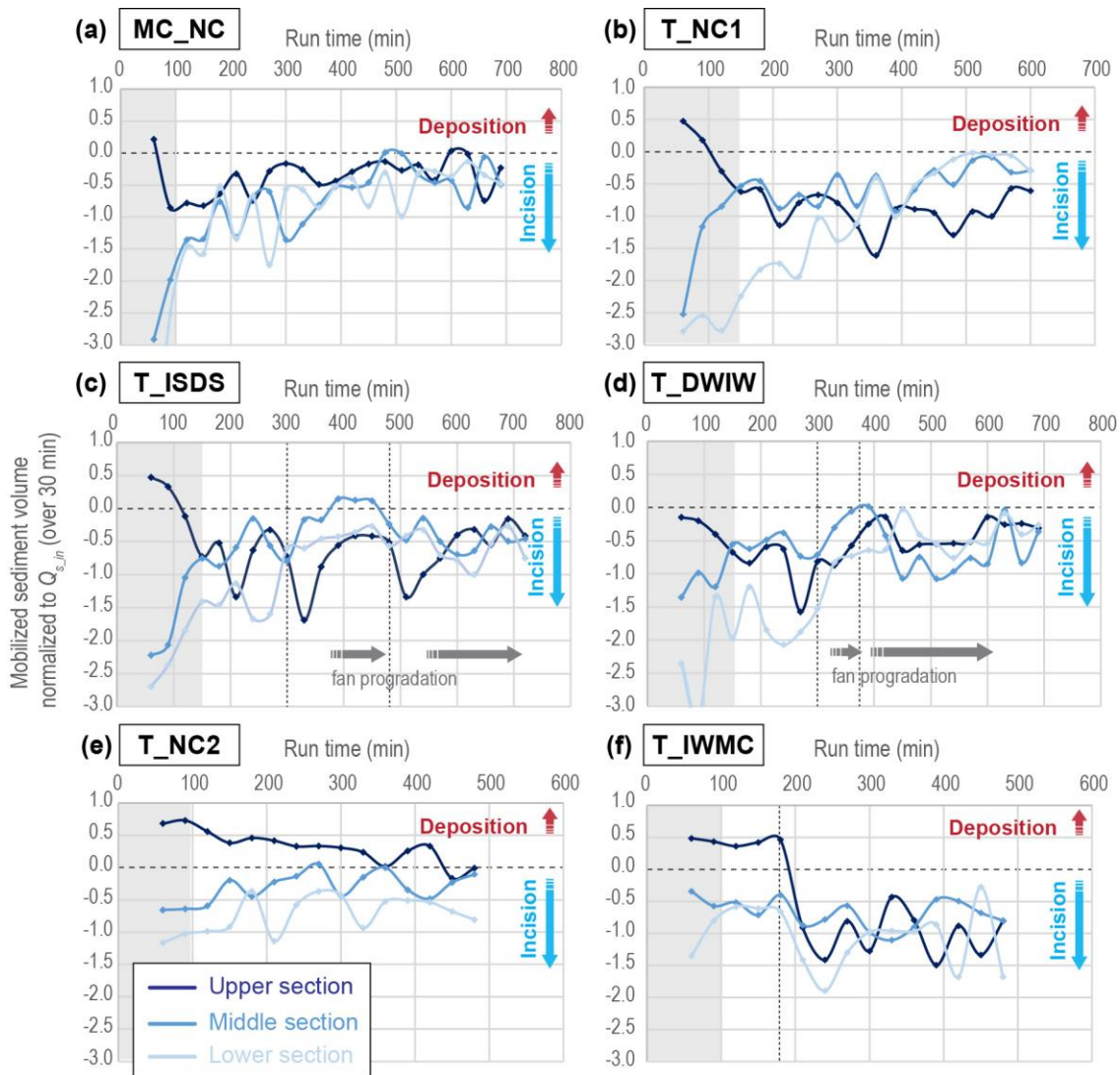
409 4.3. Downstream sediment propagation

410 To analyze the effects of the tributary on the mobility of sediment within the coupled
411 tributary–main-channel system, we monitored the volumes of sediment mobilized (V) in the
412 upper, middle, and lower sections of the fluvial network through time (Fig. 8). The complex
413 pattern of V in the different sections yields insights into downstream sediment propagation,
414 especially when coupled with maps of the spatial distribution of eroded and deposited sediment
415 (Figs. S2 to S7 in the Supp. Material):

- 416 1. In all experiments, including the one without a tributary (MC_NC), sediment moved in
417 pulses through the system (Fig. 8). As such, the mobilized volumes (V) of each section
418 can be *in-phase* or *out-of-phase* with the volumes mobilized in the others sections
419 (Castelltort and Van Den Driessche, 2003) depending on where the “pulse” of sediment
420 was located within the floodplain (Fig. 9a).
- 421 2. The sediment mobilized in the middle and lower sections of the T_NC1 run showed a
422 decrease in V after ca. 400 min, whereas in the upper section V remained nearly constant
423 (Fig. 8b), despite a marked increase in V_{vf} (Fig. S8 of Supp. Material).
- 424 3. In the T_ISDS run, the middle section showed, as expected, a strong reduction in V after
425 the onset of increased Q_{s_in} in the tributary and consequent fan aggradation (300 to 480
426 minutes). Conversely, it showed an increase in V following the decrease in Q_{s_in} and
427 consequent fan incision (480 minutes to the end of the run) (Fig. 8c). A similar pattern
428 can be seen in the lower section, with a reduction in V during fan aggradation and an
429 increase in V during fan incision. Interestingly, the upper section showed two peaks of
430 enhanced V (i.e., increase in sediment export) just after the changes in the tributary,
431 followed by a prolonged reduction of V (i.e., decrease in sediment export) during phases
432 of fan progradation.
- 433 4. Patterns similar to those described for the T_ISDS can be seen for the T_DWIW run.
434 However, due to the type of change in the tributary (i.e., decrease in Q_w , which increases
435 the Q_s/Q_w ratio, reducing the sediment-transport capacity) and due to the shorter duration
436 of the perturbation (300 to 375 minutes), the first peak of enhanced V in the upper
437 section was barely visible, whereas the second peak was not present. Rather, the upper

438 section shows a continuous decrease in V until ca. 420 min, i.e., circa 45 minutes after the
 439 the onset of increased Q_w in the tributary (Fig. 8d and Fig. S5 of Supp. Material).
 440 5. The T_NC2 experiment is dominated by aggradation and V values are rather constant;
 441 (Fig. 8e and Fig. S6 of Supp. Material). Similar to the final part of the T_NC1 run, the
 442 upper section of the main channel showed a general increasing trend in V_{vf} (Fig. S9 of
 443 Supp. Material).
 444 6. In the T_IWMC experiment, as expected, V increased immediately after the increase in
 445 Q_w in main channel in all three sections (indicating major incision), but was particularly
 446 evident in the upper and lower sections of the main channel (Fig. 8f).

447



448

449 Figure 8. Volume (V) of sediment mobilized in each section (e.g., upper, middle, and lower
450 sections). Vertical lines represent the *times of change* in boundary conditions; horizontal dashed
451 line separates aggradation and erosion.

452

453 5. Discussion

454 Our six experiments provide a conceptual framework for better understanding how tributaries
455 interact with main channels under different environmental forcing conditions (Fig. 1). We
456 particularly considered geometric variations of the two subsystems (i.e., tributaries and main
457 channels) and the effects of tributaries on the downstream delivery of sediment within the fluvial
458 system.

459 5.1. Aggrading and incising fans: geometrical adjustments and tributary–main- 460 channel interactions

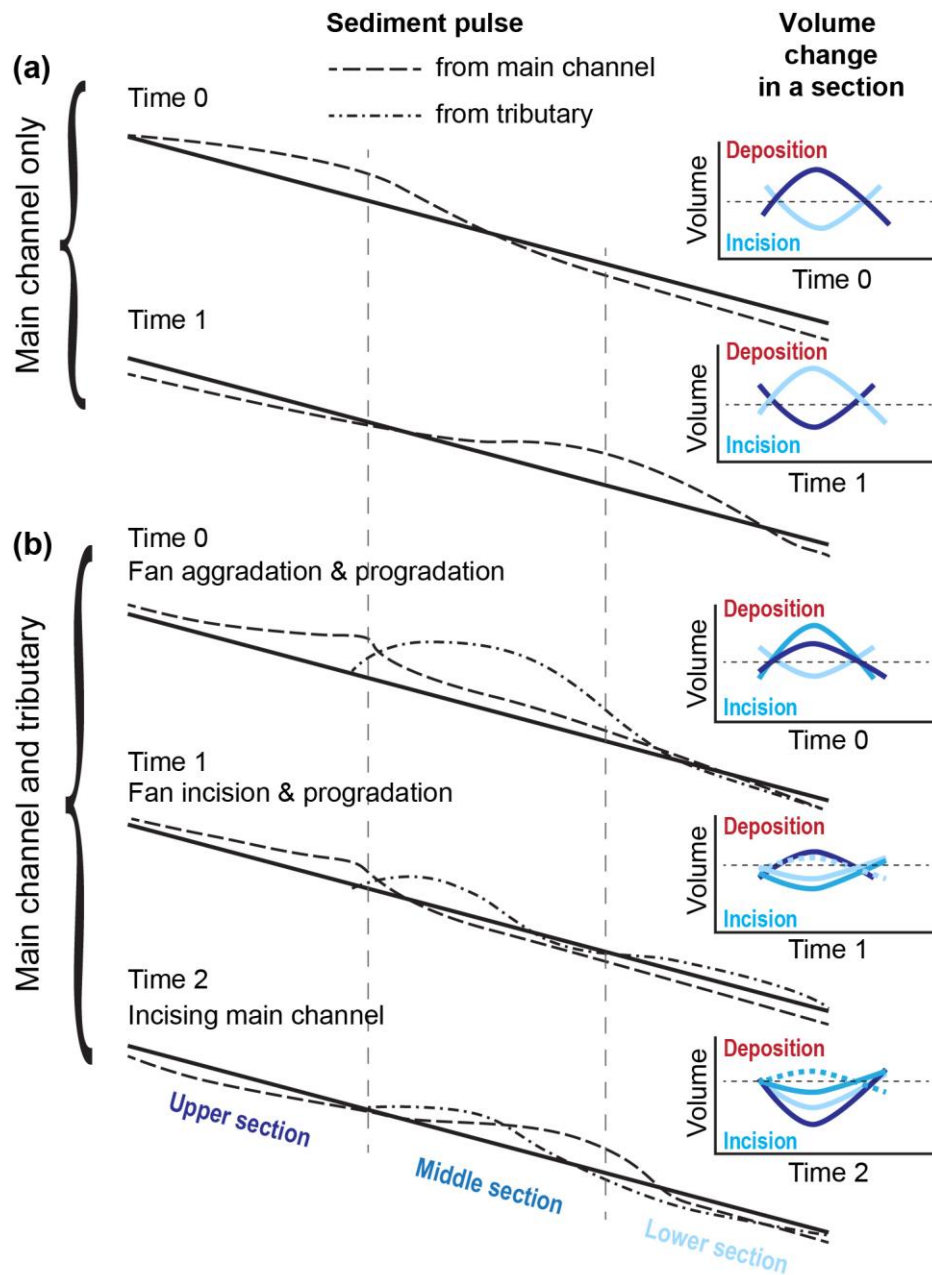
461 In our experiments, the aggrading alluvial fans strongly impacted the width of the main-
462 channel valley both upstream and downstream of the tributary junction. By forcing the main
463 channel to flow against the valley-wall opposite the tributary, bank erosion was enhanced
464 (Tables S3 to S8 and Fig. S8 in the Supp. Material), thus widening the main-channel valley floor
465 (Figs. 4, 6, and S4). Bank erosion and valley widening in the main channel also occurred during
466 periods of fan incision (Figs. S4b, S5, and S8 of the Supp. Material). We hypothesize that this
467 widening was related to pulses of sediment eroded from the fan, which periodically increased the
468 sediment load to the main channel and helped to push the river to the side opposite the tributary
469 (Grimaud et al., 2017; Leeder and Mack, 2001). Once there, the river undercut the banks,
470 causing instability and collapse. As such, periods of fan incision triggered a positive feedback
471 between increased load in the main channel and valley widening, which occurred through bank
472 erosion and bank collapses. In these scenarios, bank contribution (V_b) in the middle and lower
473 sections of the main channel can be equal to, or larger than, the sediment mobilized within the
474 active valley floor (V_{vf}) (also for the T_NC2 run; Fig. 7b and Fig. S8 and S9, Supp. Material). It
475 follows that the composition of the fluvial sediment may be largely dominated by material
476 mobilized from the valley walls, with important consequences, for example, for geochemical or
477 provenance studies (Belmont et al., 2011).

478 Our analysis of sediment mobility within the different sections of the main channel
479 highlighted that the presence of the alluvial fan affects the time needed to reach equilibrium in
480 the different reaches of the main river: in the T_NC1 run, for example, due to the sediment input
481 from the tributary, the middle and lower sections have a higher Q_s/Q_w ratio (0.022) than the
482 upper section (0.014), and may reach equilibrium faster (Gilbert, 1877; Wickert and Schildgen,
483 2019). Once the tributary channel-profile reached equilibrium (e.g., at ca. 420 minutes for
484 T_NC1; inset of Fig. 4b), the upper main channel rapidly adjusted by decreasing the elevation of
485 its channel bed (Fig. 4b) and increasing the sediment mobilized (Fig. 8b and Fig. S8 of Supp.
486 Material). This result suggests that equilibrium time scales of channels upstream and
487 downstream of tributaries can vary (Schumm, 1973), and that in a top-down direction of
488 adjustments, the equilibrium state of the upper section may be dictated by the equilibrium state
489 of its lower reaches because of the tributary influence.

490 In our experiments, fans were built under conditions that caused deposition at the tributary
491 junction (e.g., an increase in Q_{s_in} or decrease in Q_w in the tributary). When the perturbation
492 lasted long enough (e.g. in experiment T_ISDS), the fan prograded into the main channel. The
493 passage from fan aggradation to progradation was delayed relative to the onset of the
494 perturbation by the time necessary to move the sediment from the fan head to the fan margin
495 (e.g. for > 60 min in T_ISDS; Fig. S4b). This delay allowed for a temporarily efficient transfer of
496 sediment within the main channel (as marked by the peak in V of the upper main channel section;
497 Fig. 8c). For tributaries subject to a change that caused tributary incision (e.g., decrease in Q_{s_in}
498 or increase in Q_w), the elevation of the fan surface was progressively lowered (inset of Fig. 4c
499 and d, and Fig. S1 in the Supp. Material), and the fan prograded into the main channel with
500 cyclic pulses of sediment discharge (e.g., Fig. S4c) (Kim and Jerolmack, 2008). Progradation
501 was generally localized where the tributary channel debouched into the main river (e.g.,
502 depositing the *healing wedge* of Leeder and Mack, 2001), generally shortly after (< 30 min) the
503 onset of the perturbation (Figs. S4c and S5 of the Supp. Material). When the fan prograded,
504 sediment in the main channel was partially blocked above the tributary junction (e.g., at 390 to
505 480 min in Fig. S4b, and at 510 min to the end of the run in Fig. S4c; Fig. S6 of Supp. Material),
506 and the upstream main-channel section experienced a prolonged decrease in sediment mobility
507 due to localized aggradation (Fig. 8c and d, and Fig. 9b).

508 Given the relative size of the tributary and main channel in our experiments (Q_w tributary ~
509 $2/3 Q_w$ main channel) and the magnitude of the perturbations (doubling of Q_{s_in} or halving of
510 Q_w), the impact of perturbations in the tributary on the sediment mobility (V) within the main
511 channel remained mostly within autogenic variability (Fig. 7b, Group 1). This observation
512 highlights how the analysis of changes in Q_{s_out} alone (for example inferred from the stratigraphy
513 of a fluvial deposit) may not directly reflect changes that occurred in the tributary, but can be
514 overprinted by autogenic variability. However, the analysis of V within individual sections of the
515 main channel, and particularly within the confluence zone (i.e., middle section), together with the
516 analysis of how sediment moves in space, reveal important changes in the sediment dynamics of
517 the main channel that may help to reconstruct the perturbations that affected the tributary
518 (Section 5.2; Figs. 8 and 9b). This observation underscores the need to study a range of
519 sedimentary deposits of both the tributary and main-channel (Mather et al., 2017), both upstream
520 and downstream of a tributary junction.

521



522

523 Figure 9. Schematic representation of the average sediment mobilized in each section of the main
 524 channel. Solid black line represents the idealized equilibrium profile of the main channel,
 525 whereas dashed lines represent the volumes mobilized from the main channel and from the
 526 tributary. (a) Sediment dynamics in a single-channel system: sediment moves in pulses and upper
 527 and lower sections may be *out-of-phase* or *in-phase* depending on the dynamics of the middle
 528 section (i.e., the *transfer zone* of Castellort and Van Den Driessche, 2003). (b) Sediment
 529 dynamics in a tributary-main channel system: *Time 0* represents the “aggrading (and prograding)
 530 fan” scenario, where the upper and middle sections of the main channel undergo aggradation,
 531 while the lower section undergoes incision. *Time 1* represents the “incising (and prograding) fan”
 532 scenario, where the upper section may still be aggrading by it also starts to get incise creating a
 533 pulse of sediment that reaches the lower section. The middle section clearly sees an increase in

534 incision due to the imposed perturbation, while the lower section may undergo incision or
535 aggradation depending on the amount of sediment delivered from the fan, from the upper section,
536 and from bank erosion. *Time 2* represents the “incising main channel” scenario, where the fan
537 loses its influence on the dynamics of the main channel and both upper and lower sections
538 undergo incision. The middle section can undergo aggradation or incision depending on the
539 amount of sediment mobilized in the tributary and on the pulse of sediment moving from the
540 upper to the lower section of the main channel.

541

542 5.2. Incising main channel: geometric adjustments and tributary–main-channel 543 interactions

544 The main-channel bed elevation dictates the local base level of the tributary, such that
545 variations in the main-channel long profile may cause aggradation or incision in the tributary
546 (Cohen and Brierly, 2000; Leeder and Mack, 2001; Mather et al., 2017). In our experiments,
547 lowering of the main-channel bed triggered tributary incision that started at the fan toe and
548 propagated upstream (insets in Fig. 4). Because tributary incision increases the volume of
549 sediment supplied to the main channel, a phase of fan progradation would be expected, similar to
550 the cases described above (and in the *complex response* of Schumm, 1973). However, in our
551 experiment (i.e., T_IWMC), progradation did not occur: instead, the fan was shortened (Fig. S7
552 Supp. Material). We hypothesize that the increased transport capacity of the main river resulted
553 in an efficient removal of the additional sediment from the tributary, thereby mitigating the
554 impact of the increased sediment load supplied by the tributary to the main channel. Another
555 consequence is that the healing wedge of sediment from the tributary is likely not preserved in
556 the deposits of either the fan margin or the confluence zone, hindering the possibility to
557 reconstruct the changes affecting the tributary. However, some insight can be obtained from the
558 analysis of sediment mobility. During main-channel incision, whereas both upper and lower
559 sections of the main channel registered a marked increase in V following the perturbation, the
560 middle section showed only minor variations (Fig. 8f). We hypothesize that this lower variability
561 was due to the buffering effect of the increased load supplied from the fan undergoing incision
562 (i.e., caused by the sudden base-level fall that followed main-channel incision) (Fig. 9b). In
563 contrast, when incision in the tributary was caused by a perturbation in its headwaters, V initially
564 increased and then showed a prolonged decrease in the upper section during fan aggradation,
565 whereas it increased in the middle section during fan incision. These differences may help to

566 discern the cause of fan incision (i.e., either a perturbation in the main channel or in the
567 tributary).

568 We did not observe the *complex response* described by Schumm (1973), characterized by
569 tributary aggradation following incision along the main channel. The complex response in
570 Schumm's experiments likely occurred because the main river had insufficient power to remove
571 the sediment supplied by the tributaries, as opposed to what occurred in our experiments. When
572 aggradation occurs at the tributary junction, one may expect to temporarily see an evolution
573 similar to that proposed in the "aggrading alluvial fan" scenario, with the development on an
574 alluvial fan that may alter the sediment dynamics of the main channel, modulating the sediment
575 mobilized in the upper and lower sections of the river and delaying main-channel adjustments. In
576 our experiment, instead, a prolonged erosional regime within the main channel may have led to
577 fan entrenchment and fan-surface abandonment (Clarke et al., 2008; Nicholas and Quine, 2007;
578 Pepin et al., 2010; Van Dijk et al., 2012). Despite the lack of fan progradation, an increase in
579 bank contribution following incision of the main channel did occur (Fig. 7b.6, Fig. S9 Supp.
580 Material) and could be explained by (1) higher and more unstable banks and (2) an increased
581 capacity of the main channel to laterally rework sediment volumes under higher water discharges
582 (Bufe et al., 2019).

583 5.3. Sediment propagation and coupling conditions

584 Understanding the interactions between tributaries and main channel, and the contribution of
585 these two sub-system to the sediment moved (either eroded or deposited) in the fluvial system, is
586 extremely important for a correct interpretation of fluvial deposits (e.g., cut-and-fill terraces or
587 alluvial fans), which are often used to reconstruct the climatic or tectonic history of a certain
588 region (e.g., Armitage et al., 2011; Densmore et al., 2007; Rohais et al., 2012; Simpson and
589 Castellort, 2012).

590 In their conceptual model, Mather et al. (2017) indicate that an alluvial fan may act as a
591 *buffer* for sediment derived from hillslopes during times of fan aggradation, and as a *coupler*
592 during times of fan incision, thereby allowing the tributary's sedimentary signals to be
593 transmitted to the main channel. From our experiments, we can explore the effects that tributaries
594 have not only in storing or releasing sediment to the main channel, but also in modulating the
595 flux of sediment within the fluvial system. In doing so, we create a new conceptual framework

596 that takes into account the connectivity within a coupled alluvial fan-main channel system and
597 the mechanisms with which sediment and sedimentary signals may be recorded in local deposits
598 (Fig. 10). Results are summarized as follows.

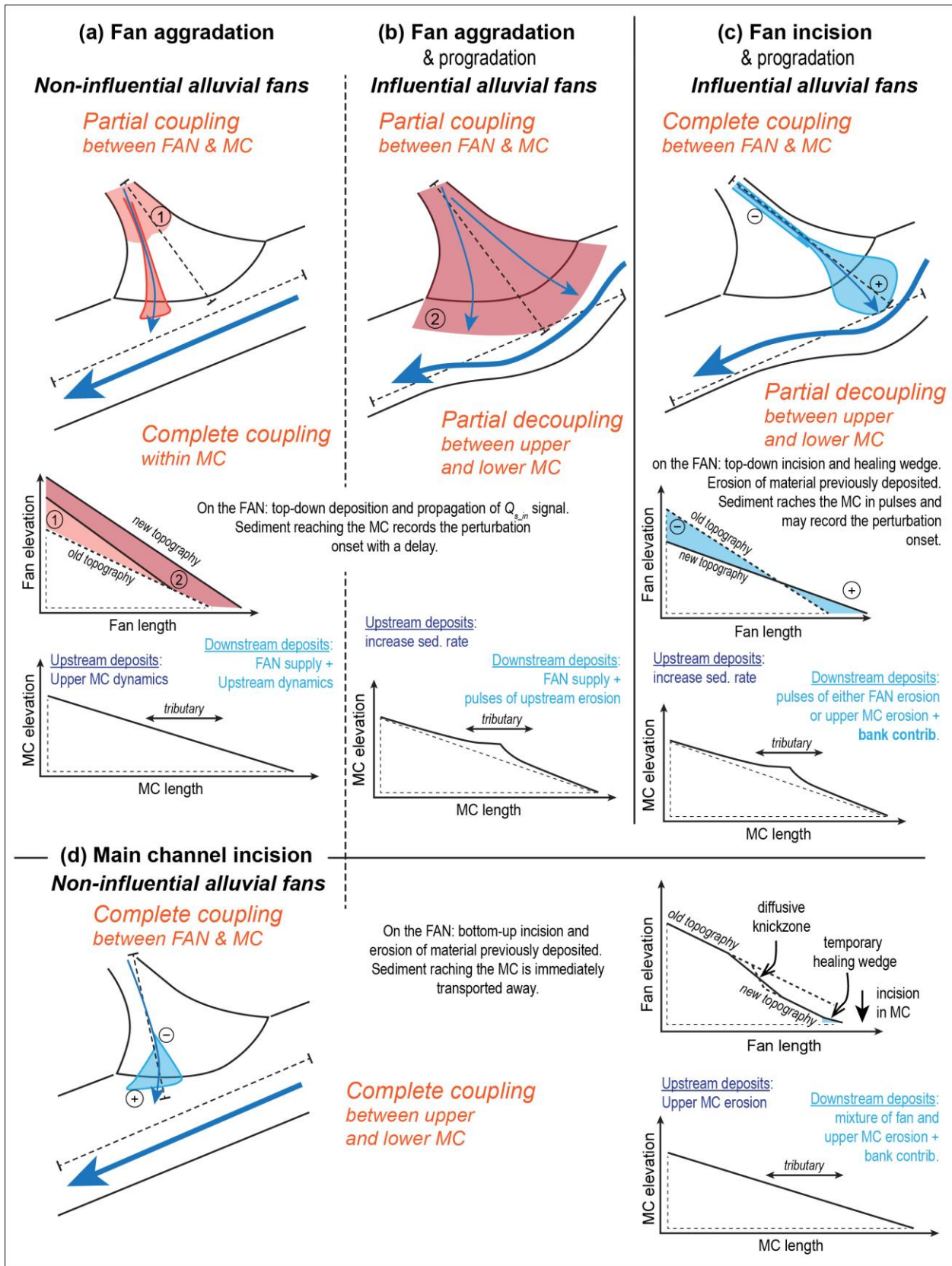
599 *5.3.1. Aggrading and incising fans*

- 600 1. If the tributary has perennial water discharge, a *partial coupling* between the tributary
601 and the main channel is possible. Also, during fan aggradation, when most of the
602 sediment is deposited and stored within the fan (e.g., Fig. S4b), a portion of the Q_{s_in}
603 reaches the main channel in proportion to the transport capacity of the tributary channel
604 (Fig. 10a and b). The partial coupling between the fan and the main channel allows for a
605 *complete coupling* between the upstream and downstream sections of the main river (Fig.
606 S4b – 300-390 min, and S5b in the Supp. Material). As such, during fan aggradation, the
607 main channel behaves as a single connected segment, and the lower section receives
608 sediment in proportion to the transport capacity of the main and tributary channels. The
609 material supplied by the tributary to the main channel is dominated by the tributary's
610 Q_{s_in} with little remobilization of previously deposited material.
- 611 2. During fan incision, large volumes of sediment are eroded from the fan and transported
612 into the main channel as healing wedges, allowing the fan to prograde into the main
613 channel (Fig. S4c and 10c). This process creates a *complete coupling* between the
614 tributary and the main channel (Fig. 8c and d), with the material supplied by the tributary
615 mostly dominated by sediment previously deposited within the fan.
- 616 3. During times of fan progradation, the fan creates an obstacle to the transfer of sediment
617 down the main channel, creating a *partial decoupling* between upstream and downstream
618 sections of the main channel (Fig. 8, S4b and c, and 10b and c). As a consequence, the
619 sediment carried by the main channel is trapped above the tributary junction and thus will
620 be missing from downstream sedimentary deposits. However, the upstream section of the
621 main channel may be periodically subject to incision (e.g., Fig. S4b and c), moving
622 mobilized sediment from the upper to the lower section. Accordingly, if progradation of
623 the fan is caused by prolonged fan aggradation, the downstream section will receive the
624 Q_{s_in} from the fan, plus pulses of sediment eroded from the upstream section of the main
625 channel. Conversely, if progradation is due to incision of the tributary and mobilization
626 of additional fan sediment, the downstream section will receive pulses of erosion from

627 either the fan or the upstream section of the main channel, plus the contribution of bank
628 erosion.

629 In summary, downstream fluvial deposits record the competition between the main
630 channel and the tributary: the alluvial fan pushes the main channel towards the opposite side
631 of the valley to adjust its length, whereas the main channel tries to maintain a straight course
632 by removing the material deposited from the fan. If the main channel dominates, it cuts the
633 fan toe and permits sediment from upstream of the junction to be more easily moved
634 downstream. If the tributary dominates, the main channel will be displaced and the transfer of
635 sediment through the junction will be disrupted. An autogenic alternation of these two
636 situations is possible, whereby fan-toe cutting may trigger fan incision and progradation,
637 increasing the influence of the fan on the main channel. The composition of the sediment
638 downstream thus reflects the competition between main channel and alluvial fan, with
639 contributions from both sub-catchments. In addition, bank erosion may make important
640 contributions to sediment supply and transport, particularly during periods of fan incision
641 (Fig. S8 in the Supp. Material). From these results, we therefore distinguish between: 1)
642 *Influential alluvial fans*, which have a strong impact on the geometry and sediment-transfer
643 dynamics of the main channel, and 2) *Non-influential alluvial fans*, which do not
644 substantially alter the geometry or sediment-transfer dynamics of the main channel.

645



647 Figure 10. Conceptual framework for the coupling conditions of an alluvial-fan/main-channel
648 (MC) system under different environmental forcings. For *aggrading and incising alluvial fans*
649 (upper panels), the fan-main channel connectivity depends on the dynamics acting in the alluvial
650 fan, being partially coupled during fan aggradation and totally coupled during fan incision. For
651 *incising main rivers* (lower panel) the fan and main channel are fully coupled. As well, *non-*
652 *influential alluvial fans* (left and lower panels) favors a complete coupling within the main
653 channel, whereas *influential alluvial fans* (middle and right upper panels) may favor a partial
654 decoupling between upstream and downstream sections of the main river. Each one of the four
655 settings presented here brings its own sedimentary signature, different responses to perturbations,
656 and dynamics of signal propagation which may be recorded into the fluvial deposits.

657

658 5.3.2. *Incising main channel*

- 659 1. Lowering of the main-channel bed triggers incision into the alluvial fan, thereby
660 promoting a *complete coupling* between the fan and the main channel (Fig. 10d, and S7
661 in the Supp. Material). The sediment supplied by the tributary is mainly composed of
662 material previously deposited within the fan.
- 663 2. An increase in main-channel water discharge increases the transport capacity of the
664 mainstem so that it persistently “wins” the competition with the alluvial fan. In this case,
665 despite the incision triggered in the alluvial fan, which increases the sediment supplied by
666 the tributary, the main channel efficiently removes the additional sediment load, thereby
667 reducing the influence of the alluvial fan on downstream sediment transport within the
668 main channel (Fig. S7 in the Supp. Material). The consequence is a *complete coupling*
669 between the upstream and downstream sections of the main channel (Fig. 10d). The
670 sediment reaching the lower section is a mixture of eroded material from the main
671 channel, within the fan, and along the banks.

672 5.4. Limitations of the experiments and implications for field studies

673 Physical experiments have the advantage of simulating many of the complexities of natural
674 systems in a simplified setting (Paola et al., 2009). Because of the simplifications, however, a
675 number of limitations arise when attempting to compare experimental results to natural
676 environments. One limitation of our study concerns the small number of experiments that we
677 have performed compared to the full variability of natural river systems and the lack of repetition
678 of experiments. This limitation prevents us, for example, from fully distinguishing significant
679 trends in sediment mobility from stochastic or autogenic processes that are inherent of alluvial

680 systems. In Section 2.2, we described how fan-toe cutting may create the same response in the
681 tributary as incision along the main channel. However, we are not able to quantify the relative
682 contribution of these two processes on the changes occurring in the tributary. One way to
683 distinguish between fan-toe cutting and main-channel incision is to study the whole fluvial
684 system, thus including all tributaries: Main channel variations will affect all tributaries with a
685 timing that is diachronous in the direction of the change (Mather et al., 2017 and references
686 therein). Fan-toe cutting, on the other hand, will be specific of single tributaries with “random”
687 timings.

688 Another limitation of our experiments relates to the *scaling*. Our experiments were not scaled
689 to any particular environment. Instead we used the principle of *similarity of processes* as
690 suggested by Hooke (1968). However, the use of a single grain size for both the tributary and the
691 main channel prevents us from analyzing geomorphic changes that are associated to the input of
692 a coarser grain size from a tributary or to the thinning of sediment in the main channel upstream
693 of the fan. In this regard, we point again to the work of Ferguson et al. (2006) which, by
694 analyzing the effects of grain-size variations on channel slope, may represent a good complement
695 to our analyses. Finally, the patterns highlighted by our experiments are partially dictated by the
696 choices made in setting the values of Q_w and Q_{s_in} , and by the timing and the magnitude of the
697 imposed perturbations.

698 Despite these shortcomings, the analysis presented here provides insights into how channels
699 respond to changes in water and sediment discharge at confluence zones, and how sediment
700 moves through branched fluvial systems. In particular, the dynamics that govern the movement
701 of sediment can have important repercussions for field studies, particularly for interpretations of
702 alluvial-channel long profiles, dating of material within stratigraphic sequences, and for
703 interpretations of their geochemical composition (e.g., Tofelde et al., 2019, and references
704 therein). Additionally, by partially decoupling the upper and lower sections of the main channel,
705 fan progradation may lead to pulses of sediment movement from the upper to the lower sections
706 of the main channel, therefore disrupting environmental signals that could be transmitted
707 downstream (e.g., Simpson and Castelltort, 2012). Indeed, the stratigraphy of the downstream
708 section of the main channel may record periods of high sedimentation rates, erroneously pointing

709 to periods of high sediment supply, when in reality the fast accumulation may be related to a
710 pulse of sediment being eroded from the upstream section of the main channel.

711 These complexities highlight the need for further research on these topics and the importance
712 of studying the coupled tributary-main channel system to fully understand the dynamics acting in
713 the river network and correctly interpret both geochemical and stratigraphic signals.

714 6. Conclusion

715 We performed six experiments to analyze the interactions of a tributary–main-channel
716 system when a tributary produces an alluvial fan. We found that differing degrees of coupling
717 may be responsible for substantial changes in the geometry of the main channel and the sediment
718 transfer dynamics of the system. In general, we found that the channel geometry (i.e., channel
719 slope and valley width) adjusts to changes in sediment and water discharge in accordance with
720 theoretical models (e.g., Ferguson and Hoey, 2008; Parker et al., 1998; Whipple et al., 1998;
721 Wickert and Schildgen, 2019). Additionally, by analyzing the effects of the tributary-main
722 channel interactions on the downstream delivery of sediment, we have shown that the fluvial
723 deposits within the main channel above and below the tributary junction may record
724 perturbations to the environmental conditions that govern the fluvial system.

725 Our main results can be summarized as follows (Fig. 10):

726 (1) Fan aggradation leads to a partial coupling between the fan and the main channel, which
727 permits a complete coupling between the main-channel reaches upstream and downstream of the
728 tributary junction. As such, the provenance of downstream sediment reflects the dynamics of
729 both sub-catchments (e.g., tributary and main river), and remobilized material from older
730 deposits will be minimal.

731 (2) Fan incision favors a complete coupling between the fan and the main channel, and
732 remobilizes material previously stored in the fan.

733 (3) Fan progradation (either during prolonged aggradation or fan incision) strongly
734 influences the main channel. As a result, the connectivity of the main river across the tributary
735 junction is reduced and the deposits of the fluvial system above and below the junction may
736 record different processes.

737 (4) Incision along the main channel triggers incision in the alluvial fan that, despite an
738 increased sediment supply to the main river, reduces its influence on the dynamics of the main
739 channel. The result is a fully connected fluvial system in which the deposits record sediment-
740 transfer dynamics and the interactions between both the alluvial fan and the main river, including
741 a large component of material remobilized from older deposits.

742 The theoretical framework proposed in this study aims to illustrate the dynamics acting
743 within a tributary junction. It provides a first-order analysis of how tributaries affect the sediment
744 delivered to the main channels and of how sediment is moved through the system under different
745 environmental forcing conditions. The (dis)connectivity within the fluvial system has important
746 consequences for the stratigraphy and architecture of depositional sinks, as it may be responsible
747 for the continuity of the sedimentary record or for the disruption of the environmental signals
748 carried through the main channel (Simpson and Castellort, 2012). Our findings may be used to
749 improve the understanding of the interactions between tributaries and main channels, providing
750 essential information for the reconstruction of the climatic or tectonic histories of a basin.

751 **Data availability**

752 Data will be made available through the Sediment Experimentalists Network Project Space to
753 the SEAD Internal Repository.

754 **Video supplement**

755 Time-lapse video of the experiment will be uploaded.

756 **Supplement**

757 Supplement tables and figures can be found in the supplementary document.

758 **Author contributions**

759 SS, ST, and ADW designed and built the experimental setup. SS and ST performed the
760 experiments. SS analyzed the data with the help of ST, ADW and AB. All authors discussed the
761 data, designed the manuscript, and commented on it. SS designed the artwork.

762

763 **Competing interests**

764 The authors declare that they have no conflict of interest.

765

766 **Acknowledgments**

767 We thank Ben Erickson, Richard Christopher, Chris Ellis, Jim Mullin, and Eric Steen for
768 their help in building the experimental setup and installing equipment. We are also thankful to
769 Jean-Louis Grimaud and Chris Paola for fruitful discussions and suggestions.

770

771 **Financial support**

772 This research has been supported by the Deutsche Forschungsgemeinschaft (grant no. SCHI
773 1241/1-1 and grant no. SA 3360/2-1), the Alexander von Humboldt-Stiftung (grant no. ITA
774 1154030 STP), and the University of Minnesota.

775

776 **References**

777 Allen, P. A.: From landscapes into geological history, *Nature*, 451, 274–276,
778 <https://doi.org/10.1038/nature06586>, 2008.
779

780 Armitage, J. J., Duller, R. A., Whittaker, A. C., and Allen, P. A.: Transformation of tectonic
781 and climatic signals from source to sedimentary archive, *Nat. Geosci.*, 4, 231–235, 2011.
782

783 Belmont, P., Gran, K.B., Schottler, S.P., Wilcock, P.R., Day, S.S., Jennings, C., Lauer, J.W.,
784 Viparelli, E., Willenbring, J.K., Engstrom, D.R., and Parker, G.: Large Shift in Source of Fine
785 Sediment in the Upper Mississippi River. *Environmental Science and Technology*, 45, 8804–
786 8810, 2011.
787

788 Benda, L.: Confluence environments at the scale of river networks. In: *River Confluences,*
789 *Tributaries and the Fluvial Network* © John Wiley & Sons, Ltd. ISBN: 978-0-470-02672-4,
790 2008.
791

792 Benda, L., Miller, D., Bigelow, P., and Andras, K.: Effects of post-wildfire erosion on
793 channel environments, Boise River, Idaho. *Forest Ecology and Management*, v. 178, 105–119,
794 [doi:10.1016/S0378-1127\(03\)00056-2](https://doi.org/10.1016/S0378-1127(03)00056-2), 2003.
795

796 Benda, L., Leroy Poff, N., Miller, D., Dunne, T., Reeves, G., Pess, G., and Pollock, M.: The
797 Network Dynamics Hypothesis: How Channel Networks Structure Riverine Habitats.
798 *BioScience*, v. 54(5), 413-427, 2004a.
799

800 Benda, L., Andras, K., Miller, D., and Bigelow, P.: Confluence effects in rivers: Interactions
801 of basin scale, network geometry, and disturbance regime. *Water Resources Research*, 40,
802 W05402, [doi:10.1029/2003WR002583](https://doi.org/10.1029/2003WR002583), 2004b.
803

804 Best, J.L.: The morphology of river channel confluences. *Progress in Physical Geography:*
805 *Earth and Environment*, v. 10(2), 157-174, <https://doi.org/10.1177/030913338601000201>, 1986.
806

807 Best, J.L.: Sediment transport and bed morphology at river channel confluences.
808 *Sedimentology*, 35,481-498, 1988.
809

810 Best, J.L., and Rhoads B.L.: Sediment transport, bed morphology and the sedimentology of
811 river channel
812 Confluences. In: *River Confluences, Tributaries and the Fluvial Network* © John Wiley &
813 Sons, Ltd. ISBN: 978-0-470-02672-4, 2008.
814

815 Bierman, P. and Steig, E. J.: Estimating rates of denudation using cosmogenic isotope
816 abundances in sediment, *Earth Surf. Proc. Land.*, 21, 125–139,
817 [https://doi.org/10.1002/\(SICI\)1096-9837\(199602\)21:2<125::AID-ESP511>3.0.CO;2-8](https://doi.org/10.1002/(SICI)1096-9837(199602)21:2<125::AID-ESP511>3.0.CO;2-8), 1996.
818

819 Brown, E. T., Stallard, R. F., Larsen, M. C., Raisbeck, G. M., and Yiou, F.: Denudation rates
820 determined from the accumulation of in situ-produced ¹⁰Be in the Luquillo Experimental Forest,
821 Puerto Rico, *Earth Planet. Sc. Lett.*, 129, 193–202, [https://doi.org/10.1016/0012-](https://doi.org/10.1016/0012-821X(94)00249-X)
822 [821X\(94\)00249-X](https://doi.org/10.1016/0012-821X(94)00249-X), 1995.

823
824 Bryant M., Falk P., and Paola C.: Experimental study of avulsion frequency and rate of
825 deposition. *Geology*; v. 23; no. 4; 365–368, 1995.
826
827 Bufe, A., Turowski, J.M., Burbank, D.W., Paola, C., Wickert, A.D., and Tofelde, S.:
828 Controls on the lateral channel migration rate of braided channel systems in coarse non-cohesive
829 sediment. *Earth Surface Processes and Landforms*, <https://doi.org/10.1002/esp.4710>, 2019.
830
831 Bull W.B.: Threshold of critical power in streams. *Geological Society of America Bulletin*,
832 Part I, v. 90, 453-464, 1979.
833
834 Castellort S., and Van Den Driessche J.: How plausible are high-frequency sediment
835 supply-driven cycles in the stratigraphic record? *Sedimentary Geology*, v. 157, 3 –13;
836 doi:10.1016/S0037-0738(03)00066-6, 2003.
837
838 Clarke L. E., Quine T.A., and Nicholas A.P.: Sediment Dynamics in Changing
839 Environments (Proceedings of a symposium held in Christchurch, New Zealand, December
840 2008). IAHS Publ. 325, 2008.
841
842 Clarke L. E., Quine T.A., and Nicholas A.P.: An experimental investigation of autogenic
843 behaviour during alluvial fan evolution. *Geomorphology*, v. 115, 278–285;
844 doi:10.1016/j.geomorph.2009.06.033, 2010.
845
846 Cohen, T.J., and Brierley, G.J.: Channel instability in a forested catchment: a case study
847 from Jones Creek, East Gippsland, Australia. *Geomorphology*, 32, 109–128, 2000.
848
849 D'Arcy, M., Roda-Boluda, D.C., Whittaker, A.C.: Glacial-interglacial climate changes
850 recorded by debris flow fan deposits, Owens Valley, California. *Quaternary Science Reviews*,
851 169, 288-311, 2017.
852
853 Dingle, E. H., Attal, M., and Sinclair, H. D.: Abrasion-set limits on Himalayan gravel flux,
854 *Nature*, 544, 471–474, 5 <https://doi.org/10.1038/nature22039>, 2017.
855
856 De Haas T., Van den Berg W., Braat L., and Kleinhans M.G.: Autogenic avulsion,
857 channelization and backfilling dynamics of debris-flow fans. *Sedimentology*, v. 63, 1596–1619.
858 Doi; 10.1111/sed.12275, 2016.
859
860 Densmore A.L., Allen P.A., and Simpson G.: Development and response of a coupled
861 catchment fan system under changing tectonic and climatic forcing. *J. Geophys. Res.*, 112,
862 F01002, doi:10.1029/2006JF000474, 2007
863
864 Faulkner, D.J., Larson, P.H., Jol, H.M., Running, G.L., Loope, H.M., and Goble, R.J.:
865 Autogenic incision and terrace formation resulting from abrupt late-glacial base-level fall, lower
866 Chippewa River, Wisconsin, USA. *Geomorphology*, v. 266, 75–95,
867 <http://dx.doi.org/10.1016/j.geomorph.2016.04.016>, 2016.
868

869 Ferguson, R.I., Cudden, J.R., Hoey, T.B., and Rice, S.P.: River system discontinuities due to
870 lateral inputs: generic styles and controls. *Earth Surf. Process. Landforms*, v. 31, 1149–1166, doi:
871 10.1002/esp.1309, 2006.

872

873 Ferguson, R.I., and Hoey, T.: Effects of tributaries on main-channel geomorphology. In:
874 *River Confluences, Tributaries and the Fluvial Network* © John Wiley & Sons, Ltd. ISBN: 978-
875 0-470-02672-4, 2008.

876

877 Gao L., Wang X., Yi S., Vandenberghe J., Gibling M.R., and Lu H.: Episodic Sedimentary
878 Evolution of an Alluvial Fan (Huangshui Catchment, NE Tibetan Plateau). *Quaternary*, v. 1(16);
879 doi:10.3390/quat1020016, 2018.

880

881 Germanoski, D., Ritter, D.F.: Tributary response to local base level lowering below a dam.
882 *Regulated rivers: research and management*, v. 2, 11-24, 1988.

883

884 Gilbert, G. K.: Report on the Geology of the Henry Mountains, US Gov. Print. Off.,
885 Washington, D.C., USA, <https://doi.org/10.3133/70038096>, 1877.

886

887 Giles P.T., Whitehouse B.M., and Karymbalis E.: Interactions between alluvial fans and
888 axial rivers in
889 Yukon, Canada and Alaska, USA. From: Ventra, D. & Clarke, L. E. (eds) *Geology and*
890 *Geomorphology of Alluvial and Fluvial Fans: Terrestrial and Planetary Perspectives*. Geological
891 Society, London, Special Publications, v. 440; <http://doi.org/10.1144/SP440.3>, 2016.

892

893 Gippel, C.: Changes in stream channel morphology at tributary junctions, Lower Hunter
894 Valley,
895 New South Wales. *Australian GeOgphiCQI Studies*, v. 23, 291-307, 1985.

896

897 Grant, G.E., and Swanson, F.J.: Morphology and Processes of Valley Floors in Mountain
898 Streams,
899 Western Cascades, Oregon. *Natural and Anthropogenic Influence in Fluvial*
900 *Geomorphology*, Geophysical Monograph, 89, 1995.

901

902 Granger, D. E., Kirchner, J. W., and Finkel, R.: Spatially averaged long-term erosion rates
903 measured from in situ-produced cosmogenic nuclides in alluvial sediment, *J. Geol.*, 104, 249–
904 257, 1996.

905

906 Heine, R.A., and Lant, C.L.: Spatial and Temporal Patterns of Stream Channel Incision in
907 the Loess Region of the Missouri River, *Annals of the Association of American Geographers*,
908 99(2), 231-253, DOI: 10.1080/00045600802685903, 2009.

909

910 Hamilton P.B., Strom K., and Hoyal D.C.J.D.: Autogenic incision-backfilling cycles and
911 lobe formation during the growth of alluvial fans with supercritical distributaries.
912 *Sedimentology*, v, 60, 1498–1525; doi: 10.1111/sed.12046, 2013.

913

914 Hooke R.L.: Model Geology: Prototype and Laboratory Streams: Discussion. Geological
915 Society of America Bulletin, v. 79, 391-394, 1968.
916

917 Hooke R.L., and Rohrer W.L.: Geometry of alluvial fans: effect of discharge and sediment
918 size. Earth Surface Processes, v. 4, 147-166, 1979.
919

920 Kim W., and Jerolmack D.J.: The Pulse of Calm Fan Deltas. The Journal of Geology, 11(4),
921 315-330; <http://dx.doi.org/10.1086/588830>, 2008.
922

923 Lane, E. W.: Importance of fluvial morphology in hydraulic engineering, Proceedings of the
924 American Society of Civil Engineers, 81, 1–17, 1955.
925

926 Larson P.H., Dorn R.I., Faulkner D.J., and Friend d.A.: Toe-cut terraces: A review and
927 proposed criteria to differentiate from traditional fluvial terraces. Progress in Physical
928 Geography, v. 39(4), 417–439, 2015.
929

930 Leeder M.R., and Mack G.H.: Lateral erosion (“toe-cutting”) of alluvial fans by axial rivers:
931 implications for basin analysis and architecture. Journal of the Geological Society, London, v.
932 158, 885-893, 2001.
933

934 Leopold, L.B., and Maddock, T. Jr.: The Hydraulic Geometry of Stream Channels and Some
935 Physiographic Implications. Geological survey professional paper 252, 1953.
936

937 Lupker, M., Blard, P., Lavé, J., France-Lanord, C., Leanni, L., Puchol, N., Charreau, J., and
938 Bourlès, D.: ¹⁰Be-derived Himalayan denudation rates and sediment budgets in the Ganga basin.
939 Earth and Planetary Science Letters, 333–334, 146–156, doi:
940 <http://dx.doi.org/10.1016/j.epsl.2012.04.020>, 2012.
941

942 Mackin J.H.: Concept of the graded river. Bulletin of the Geological Society of America, v.
943 69, 463-512, 1948.
944

945 Mather A.E., Stokes M., and Whitfield E.: River terraces and alluvial fans: The case for an
946 integrated Quaternary fluvial archive. Quaternary Science Reviews, v. 166, 74-90;
947 <http://dx.doi.org/10.1016/j.quascirev.2016.09.022>; 2017.
948

949 Meyer-Peter, E. and Müller, R.: Formulas for Bed-Load Transport, in: 2nd Meeting of the
950 International Association for Hydraulic Structures Research, 7–9 June 1948, Stockholm,
951 Sweden, International
952 Association for Hydraulic Structures Research, 39–64, 1948.
953

954 Miller, J.P.: High Mountain Streams: Effects of Geology on Channel Characteristics and
955 Bed Material. State bureau of mines and mineral resources New Mexico institute of mining and
956 technology Socorro, New Mexico. Memoir 4, 1958.
957

958 Mouchéné, M., van der Beek, P., Carretier, S., and Mouthereau, F.: Autogenic versus
959 allogenic controls on the evolution of a coupled fluvial megafan–mountainous catchment system:

960 numerical modelling and comparison with the Lannemezan megafan system (northern Pyrenees,
961 France). *Earth Surf. Dynam.*, 5, 125–143, doi:10.5194/esurf-5-125-2017, 2017.

962
963 Nicholas, A.P., Quine, T.A.: Modeling alluvial landform change in the absence of external
964 environmental forcing. *Geology*, v. 35(6), 527–530; doi: 10.1130/G23377A.1, 2007.

965
966 Nicholas, A. P., Clarke L., and Quine T. A.: A numerical modelling and experimental study
967 of flow width dynamics on alluvial fans. *Earth Surf. Process. Landforms* 34, 1985–1993;
968 DOI: 10.1002/esp.1839;, 2009.

969
970 Paola, C., Straub, K., Mohrig, D., and Reinhardt L.: The “unreasonable effectiveness” of
971 stratigraphic and geomorphic experiments. *Earth-Science Reviews*, v. 97(1–4), 1-43,
972 <https://doi.org/10.1016/j.earscirev.2009.05.003>, 2009.

973
974 Parker, G.: Hydraulic geometry of active gravel rivers, *J. Hydraul. Div.*, 105, 1185–1201,
975 1978.

976
977 Parker, G.: Progress in the modeling of alluvial fans, *Journal of Hydraulic Research*, 37(6),
978 805-825, <http://dx.doi.org/10.1080/00221689909498513>, 1999.

979
980 Parker, G. Paola, C., Whipple, K.X., and Mohrig, D.: Alluvial fans formed by channelized
981 fluvial
982 And sheet flow. I: Theory. *Journal of Hydraulic Engineering*, v. 124(10), 1998.

983
984 Pepin, E., Carretier, S., and Herail, G.: Erosion dynamics modelling in a coupled catchment–
985 fan system with constant external forcing. *Geomorphology*, v. 122, 78–90,
986 doi:10.1016/j.geomorph.2010.04.029, 2010.

987
988 Reitz, M.D., Jerolmack, D.J., and Swenson J.B.: Flooding and flow path selection on
989 alluvial fans and deltas. *Geophysical Research Letters*, v. 37, L06401,
990 doi:10.1029/2009GL041985, 2010.

991
992 Reitz, M.D., and Jerolmack, D.J.: Experimental alluvial fan evolution: Channel dynamics,
993 slope controls, and shoreline growth. *Geophysical Research Letters*, v. 117, F02021,
994 doi:10.1029/2011JF002261, 2012.

995
996 Rice, S.P., and Church, M.: Longitudinal profiles in simple alluvial systems. *Water*
997 *Resources Research*, v. 37(2), 417-426, 2001.

998
999 Rice, S.P., Kiffney, P., Greene, C., and Pess, G.R.: The ecological importance of tributaries
1000 and confluences. In: *River Confluences, Tributaries and the Fluvial Network* © John Wiley &
1001 Sons, Ltd. ISBN: 978-0-470-02672-4, 2008.

1002
1003 Ritter, J.B., Miller, J.R., Enzel, Y., and Wells, S.G.: Reconciling the roles of tectonism and
1004 climate in Quaternary alluvial fan evolution. *Geology*, v. 23(3), 245–248, 1995.

1005

1006 Rohais, S., Bonnet, S., and Eschard, R.: Sedimentary record of tectonic and climatic
1007 erosional perturbations in an experimental coupled catchment-fan system. *Basin Research*, v. 24,
1008 198–212, doi: 10.1111/j.1365-2117.2011.00520.x, 2012.

1009

1010 Savi, S., Norton, K. P., Picotti, V., Akçar, N., Delunel, R., Brardinoni, F., Kubik, P., and
1011 Schlunegger, F.: Quantifying sediment supply at the end of the last glaciation: Dynamic
1012 reconstruction of an alpine debris-flow fan, *GSA Bull.*, 126, 773–790,
1013 <https://doi.org/10.1130/B30849.1>, 2014.

1014

1015 Savi, S., Schildgen T. F., Tofelde S., Wittmann H., Scherler D., Mey J., Alonso R. N., and
1016 Strecker M. R.: Climatic controls on debris-flow activity and sediment aggradation: The Del
1017 Medio fan, NW Argentina, *J. Geophys. Res. Earth Surf.*, 121, 2424–2445,
1018 doi:10.1002/2016JF003912, 2016.

1019

1020 Schildgen, T. F., Robinson, R. A. J., Savi, S., Phillips, W. M., Spencer, J. Q. G., Bookhagen,
1021 B., Scherler, D., Tofelde, S., Alonso, R. N., Kubik, P. W., Binnie, S. A., and Strecker, M. R.:
1022 Landscape response to late Pleistocene climate change in NW Argentina: Sediment flux
1023 modulated by basin geometry and connectivity, *J. Geophys. Res.-Earth*, 121, 392–414,
1024 <https://doi.org/10.1002/2015JF003607>, 2016.

1025

1026 Schumm, S. A.: Geomorphic thresholds and complex response of drainage systems, *Fluv.*
1027 *Geomorphol.*, 6, 69–85, 1973.

1028

1029 Schumm, S. A. and Parker, R. S.: Implication of complex response of drainage systems for
1030 Quaternary alluvial stratigraphy, *Nat. Phys. Sci.*, 243, 99–100, 1973.

1031

1032 Schwanghart, W. and Scherler, D.: Short Communication: TopoToolbox 2 – MATLAB-
1033 based software for topographic analysis and modeling in Earth surface sciences, *Earth Surf.*
1034 *Dynam.*, 2, 1-7, <https://doi.org/10.5194/esurf-2-1-2014>, 2014.

1035

1036 Simon, A., and Rinaldi, M.: Channel instability in the loess area of the midwestern United
1037 States. *Journal of the American Water Resources Association*, v. 36(1), Paper No. 99012, 2000.

1038

1039 Straub, K.M., Paola, C., Mohrig, D., Wolinsky, M.A., and George, T.: Compensational
1040 stacking of channelized sedimentary deposits. *Journal of Sedimentary Research*, v. 79, 673–688,
1041 doi: 10.2110/jsr.2009.070, 2009.

1042

1043 Tofelde, S., Savi, S., Wickert, A. D., Bufe, A., and Schildgen, T. F.: Alluvial channel
1044 response to environmental perturbations: fill-terrace formation and sediment-signal disruption,
1045 *Earth Surf. Dynam.*, 7, 609-631, <https://doi.org/10.5194/esurf-7-609-2019>, 2019.

1046

1047 Van den Berg van Saparoea, A.P. H., and Postma, G.: Control of climate change on the yield
1048 of river systems, *Recent Adv. Model. Siliciclastic Shallow-Marine Stratigr. SEPM Spec. Publ.*,
1049 90, 15–
1050 33, 2008.

1051

1052 Van Dijk, M., Postma, G., and Kleinans, M.G.: Autocyclic behaviour of fan deltas: an
1053 analogue experimental study. *Sedimentology*, v. 56, 1569–1589, doi: 10.1111/j.1365-
1054 3091.2008.01047.x, 2009.

1055

1056 Van Dijk, M., Kleinans, M.G., Postma, G., and Kraal, E.: Contrasting morphodynamics in
1057 alluvial fans and fan deltas: effect of the downstream boundary. *Sedimentology*, v. 59, 2125–
1058 2145 doi: 10.1111/j.1365-3091.2012.01337.x, 2012.

1059

1060 Von Blanckenburg, F.: The control mechanisms of erosion and weathering at basin scale
1061 from cosmogenic nuclides in river sediment. *Earth and Planetary Science Letters*, v. 237, 462–
1062 479, 2005.

1063

1064 Whipple, K.X., Parker, G. Paola, C., and Mohrig, D.: Channel Dynamics, Sediment
1065 Transport, and the Slope of Alluvial Fans: Experimental Study. *The Journal of Geology*, v. 106,
1066 677–693, 1998.

1067

1068 Whipple, K.X., and Tucker, G.E.: Implications of sediment-flux-dependent river incision
1069 models for landscape evolution. *Journal of Geophysical Research*, 107, B2, 2039, doi:
1070 10.1029/2000JB000044, 2002.

1071

1072 Wickert, A. D. and Schildgen, T. F.: Long-profile evolution of transport-limited gravel-bed
1073 rivers, *Earth Surf. Dynam.*, 7, 17–43, <https://doi.org/10.5194/esurf-7-17-2019>, 2019.

1074

1075 Wittmann, H., and von Blanckenburg, F.: Cosmogenic nuclide budgeting of floodplain
1076 sediment transfer. *Geomorphology*, 109, 246-256, 2009.

1077

1078 Wittmann, H., von Blanckenburg, F., Maurice, L., Guyot, J., Filizola, N., and Kubik, P.W.:
1079 Sediment production and delivery in the Amazon River basin quantified by in situ-produced
1080 cosmogenic nuclides and recent river loads. *GSA Bulletin*, 123 (5-6), 934–950, doi:
1081 <https://doi.org/10.1130/B30317.1>, 2011.

1082